Biomaterials 205 (2019) 64–80

Contents lists available at ScienceDirect

Biomaterials

journal homepage: www.elsevier.com/locate/biomaterials

Substrate mechanics controls adipogenesis through YAP phosphorylation by dictating cell spreading

Jorge Oliver-De La Cruz[a,b], Giorgia Nardone[a], Jan Vrbsky[a], Antonio Pompeiano[a], Ana Rubina Perestrelo[a], Francesco Capradossi[a], Katarína Melajová[a], Petr Filipensky[d], Giancarlo Forte[a,b,c,*]

[a] International Clinical Research Center (FNUSA-ICRC), St. Anne's University Hospital, Brno, Czech Republic
[b] Competence Center for Mechanobiology in Regenerative Medicine, INTERREG ATCZ133, Brno, Czech Republic
[c] Department of Biomaterials Science, Institute of Dentistry, University of Turku, Turku, Finland
[d] St. Anne's University Hospital, Brno, Czech Republic

ARTICLE INFO

Keywords:
Cell-matrix interaction
Mechanobiology
Adipogenesis
Mesenchymal stem cells
Biocompatible hydrogels
Cell micropatterning
YAP
Mechanosensing

ABSTRACT

The mechanoregulated proteins YAP/TAZ are involved in the adipogenic/osteogenic switch of mesenchymal stem cells (MSCs).

MSC fate decision can be unbalanced by controlling substrate mechanics, in turn altering the transmission of tension through cell cytoskeleton. MSCs have been proposed for orthopedic and reconstructive surgery applications. Thus, a tight control of their adipogenic potential is required in order to avoid their drifting towards fat tissue. Substrate mechanics has been shown to drive MSC commitment and to regulate YAP/TAZ protein shuttling and turnover. The mechanism by which YAP/TAZ co-transcriptional activity is mechanically regulated during MSC fate acquisition is still debated.

Here, we design few bioengineering tools suited to disentangle the contribution of mechanical from biological stimuli to MSC adipogenesis. We demonstrate that the mechanical repression of YAP happens through its phosphorylation, is purely mediated by cell spreading downstream of substrate mechanics as dictated by dimensionality. YAP repression is sufficient to prompt MSC adipogenesis, regardless of a permissive biological environment, TEAD nuclear presence or focal adhesion stabilization.

Finally, by harnessing the potential of YAP mechanical regulation, we propose a practical example of the exploitation of adipogenic transdifferentiation in tumors.

1. Introduction

Cells are constantly exposed to mechanical forces arising from the extracellular environment. Along with the biochemical properties of the cell niche *in vivo*, the mechanical and nanotopography cues impact on cell survival and function [1,2].

The transmission of mechanical information to the inner part of the cell, the nucleus, is achieved by a dynamic regulation of cytoskeleton integrity and tension [3].

In vitro simplified models have been lately proposed with the aim of mimicking the mechano-physical properties of *in vivo* niche [4], trying to isolate the pure effects of mechanics on cell behaviour. Indeed, such tools provided evidence that the mechanical properties of the milieu affect fundamental cellular programs involved in proliferation [5], migration [6] and differentiation [2].

In this context, a preferential commitment of mesenchymal stem cells (MSCs) towards adipogenic or osteoblastic phenotype was achieved by controlling substrate mechanics, nanotopography or cell spreading [7–10]: conditions inducing low cytoskeletal tension, such as cell confinement and compliant substrates, enhance adipogenic differentiation, while higher cell spreading and stiffer surfaces are correlated with the production of osteoblasts.

A complex network of mechanosensitive proteins displays modifications of their structure or function in response to mechanical forces. In turn, mechano-regulated proteins transduce the information into a biological response by shaping cell genetic profile and, finally, function.

Among the mechano-regulated intracellular molecular systems, Hippo pathway consists in a cascade of kinases that finally regulates the

* Corresponding author. Center for Translational Medicine (CTM), International Clinical Research Center (ICRC), St. Anne's University Hospital, Pekarska 53, Brno, 65691, Czech Republic.
E-mail address: giancarlo.forte@fnusa.cz (G. Forte).

https://doi.org/10.1016/j.biomaterials.2019.03.009
Received 9 November 2018; Received in revised form 1 March 2019; Accepted 10 March 2019
Available online 16 March 2019

phosphorylation status of Yes associated protein (YAP) and WW domain-containing transcription regulator protein 1 (WWTR1/TAZ) [11]. Following their phosphorylation by upstream kinases, Hippo effectors are sequestered in the cytoplasm and/or degraded; non-phosphorylated proteins can, instead, shuttle to the nucleus, where they act as co-transcriptional activators [12]. YAP/TAZ do not possess an intrinsic ability to bind to DNA. Thus, they dock to cell- and stage-specific transcription factors to build up functional transcriptional complexes. Among the transcription factors identified as YAP/TAZ interactors, the most characterized family is represented by TEA domain transcription factors (TEAD) [13–15].

The nuclear presence and the transcriptional activity of YAP and TAZ can be modulated by mechanical cues: substrate mechanics [7,16], fluid flow-induced shear stress [6,17], cell spreading [16,18], stretching [19] and nanopatterning [8] have all been shown to regulate YAP/TAZ localization and function.

Moreover, YAP/TAZ activity has been associated with the ability of MSCs to switch between the osteogenic and adipogenic phenotypes [7,20]. An activation of the Hippo kinases and concomitant reduction of YAP nuclear activity is observed during adipogenesis *in vitro* [21]. Nevertheless, the mechanism by which YAP/TAZ co-transcriptional activity is mechanically regulated during MSC fate acquisition is still debated.

MSCs are versatile adult stem cells with the potential to generate cells of the mesodermal lineage, including osteoblasts, chondrocytes and adipocytes. For this reason, they have been proposed for a number of clinical applications, including those related to orthopedics and reconstructive surgery [22]. Therefore, the tight control of their phenotype is of outmost importance.

Several regenerative medicine approaches have been lately proposed that exploit the osteogenic or chondrogenic differentiation of MSCs [23,24], with adipogenesis being considered a non-desired side effect of the procedure.

On the other hand, directing MSCs to adipogenic differentiation may instead be beneficial in cases when reconstructive surgery is required after cancer surgical removal [25].

In all these scenarios, the possibility to use biomaterials to fine tune implanted MSC fate and function is of great appeal since it opens the way to the setup of innovative materials-based clinical applications.

In the present study, we took advantage of a number of bioengineering platforms suited to investigate the pure effect of substrate mechanics on human MSC adipogenic commitment. In particular, we exploited unique micropatterns designed for single cell analysis, 2D and 3D hydrogels with controlled physiological Young Modulus in order to elucidate the possibility that the mechanically-induced MSC commitment is driven by YAP.

We provide evidence that YAP nuclear exclusion through its phosphorylation, as determined by a reduction in cytoskeleton tension and cell spreading, provides the mechanical imprinting needed for MSC adipogenic differentiation. YAP-mediated mechanical regulation of adipogenesis is largely independent of TEAD transcription activity: TEAD proteins are shown to have no mechanical sensitivity.

The mechanism by which YAP is excluded from the nucleus during the mechanically-driven adipogenic commitment of MSCs appears to be mediated by a combinatorial effect of F-actin remodeling and the tension produced by Myosin II motor protein. Therefore, by ruling out the contribution of focal adhesion dynamics to the mechanical regulation of adipogenesis, we demonstrate that the mechanical control of YAP co-transcriptional activity alone is sufficient to regulate adipogenic differentiation as a result of cell spreading downstream of substrate mechanics and regardless of dimensionality. Finally, to further highlight the potential clinical relevance of materials-based control of cell mechanosensitive pathways, we mechanically impaired YAP activity in breast cancer cells and demonstrated it is indeed possible to turn these cells into non-proliferative adipocytes [26].

While emphasizing the importance of the mechanical control of cell phenotype and fate, these results pave the way to materials-based therapies for different pathological conditions.

2. Materials and methods

2.1. Cell culture and treatments

ASC52telo, hTERT immortalized adipose derived Mesenchymal stem cells (AD-MSCs, ATCC® SCRC-4000™) were purchased from American Type Culture Collection (ATCC, Manassas, USA). Primary non-immortalized AD-MSCs were obtained from Lonza (Basel, Switzerland). Both primary and immortalized cells were cultured in Dulbecco's modified Eagle's medium 4.5 g/L Glucose (DMEM high Glucose, Lonza) supplemented with 10% fetal bovine serum (FBS), 2 mM L-glutamine and 100 U/ml penicillin/streptomycin.

Adipogenic differentiation was induced by seeding cells at a density of 37.500 cells/cm^2, and exposing them to adipogenic differentiation medium (ThermoFisher Scientific). Medium was changed every third day.

For the described pharmacological treatments, the following reagents were used: XMU-MP-1, Super-TDU (Selleckchem), Cytochalasin D, (−)-Blebbistatin or $MnCl_2$ (Sigma Aldrich). Chemicals were applied for 24 h in normal medium or for 72 h during adipogenic induction. The results of each experiment were compared with control preparations treated with the corresponding vehicle. For Blebbistatin and XMU-MPU-1 experiments, the medium was changed 4 h before fixation to avoid the occurrence of autofluorescence.

Cell cycle arrest was achieved by treating floating MSCs with Mitomycin C (10 μg/ml, Sigma Aldrich) for 24 h. After that period, cells were washed, seeded and exposed to adipogenic medium for 3 days.

CAL51 breast cancer cells were a gift of Dr L. Krejčí (Department of Biology, Masaryk University). Cells were cultured in DMEM medium 4.5 g/L Glucose (DMEM high Glucose, Lonza, Basel, Switzerland) supplemented with 10% fetal bovine serum (FBS), 2 mM L-glutamine and 100 U/ml penicillin/streptomycin. The YAP-deficient CAL51 line was obtained by CRISPR/Cas9 as previously described [16]. Adipogenesis was induced by seeding the cells at a density of 15000 cells/cm^2 and by switching to adipogenic differentiation medium after 24 h (ThermoFisher Scientific). Medium was changed every second day.

2.2. Cell substrate preparation and coating

Fibronectin-coated micropatterned slides with different area, shape or pattern for single cell analysis were purchased from CYTOO (ref: 10-950-10-18; 10-950-00-18). Cell suspension at a concentration of 2×10^4 cells/cm^2 was applied directly on the slides and then cultured as described above.

For the inhibition of focal adhesion formation, glass coverslips were coated overnight with a 1 mg/ml solution of high molecular weight Poly-L-Lysine (Sigma-Aldrich) at 37 °C and washed with water twice before cell seeding.

Polydimethylsiloxane (PDMS) high elastically supported surface corresponding to 1.5 and 28 kPa (μ-Dish 35 mm, IBIDI) were coated with Fibronectin solution (3 or 30 μg/ml in PBS, Stem Cells Technology) for 30 min and washed with PBS before seeding the cells.

2.3. Fibrin gel preparation

Fibrinogen (100 mg/ml) and Thrombin stocks (500 U/ml in 40 mM $CaCl_2$) (Sigma Aldrich) were mixed to produce 50 μl of softer (about 300 Pa, 5 mg/ml of fibrinogen and 2 units/ml thrombin) and stiffer (around 5 KPa, 50 mg/ml and 50 units/ml) hydrogels [27] in the presence of 16 TIU/ml of aprotinin (Sigma Aldrich). The components were allowed to polymerize at room temperature for 30 min. For 2D experiments, cells were seeded on top of the gelified hydrogel, while for 3D experiments, cells were pre-diluted in the thrombin solution so to

have them embedded when the mixture is polymerized. 25000 MSCs were used in each gel. After gelification, media with 16 TIU/ml of aprotinin and with or without XMU-MPU-1 was added to the gels. After 24 h, cells seeded for adipogenesis were changed to adipogenic media and left for 3 days.

2.4. Poly(ethylene glycol) hydrogels preparation

Functionalized poly (ethylene glycol, PEG) hydrogels were purchased from QGel (Basel, Switzerland). 15 μl gels containing 7500 cells were casted in non-coated Angiogenesis μ-Slides (IBIDI) according to manufacturer's instructions. Two pairs of formulations were chosen: gels with the same ligand density but different Young Modulus values (NS02-2, soft, 250–450 Pa; NS09-A, stiff, 900–1500 Pa), and two gels with same Young Modulus values but different ligand densities (NS25-A, low ligand density; NS84-A, high ligand density). After gelification, medium was added to the cellularized gels. When indicated, gels seeded for adipogenesis experiments were switched to adipogenic media after 24 h and fixed at day 3 for analysis.

2.5. Plasmid transfection and lentiviral production

Transient transfections were performed using Lipofectamine 3000 (Thermo Fisher Scientific) following manufacturer's recommendations. The plasmids 2 × FLAGhYAP1-S127A (17790, gift from Marius Sudol), pLX304-YAP1_PDZ (59147, gift from William Hahn), pCMV-Flag-YAP-5SA/S94A (33103, gift from, Kunliang Guan), pcDNA3-EGFP (13031, gift from Doug Golenbock) were acquired from ADDGENE repository. After transfection, the cells were left untouched for 24 h before adipogenic differentiation medium was added.

Second-generation lentiviral particles were generated by transient co-transfection of 293 T cells with a three-plasmid combination (pMD2.G, Addgene #12259; psPAX2, Addgene #12260; and either FLAG-YAP2 (8SA)-pcw10, Addgene #64637 or YAP-TEAD reporter, Addgene #68714) using FuGENE (Roche). Supernatants were collected every 24 h until day 3 after transfection and pooled together. Viral supernatant was applied for 4 h to 50% confluent AD-MSCs in the presence of 8 μg/ml polybrene (Santa Cruz Biotechnology). Two days after infection, infected cells were selected by adding 2 μg/ml puromycin (Santa Cruz Biotechnology) or by sorting GFP-positive cells.

2.6. Immunocytochemical staining

Cells were fixed with 4% paraformaldehyde for 15 min, washed with PBS, permeabilized with phosphate-buffered saline containing 0.1% Triton X (PBS-Tx-0.1%) and blocked in PBS with 2.5% bovine serum albumin for 30 min. Cells were incubated for 1 h with primary antibodies (mouse anti-YAP (Santa Cruz), mouse *anti*-vinculin (Sigma), rabbit anti-YAP, rabbit *anti*-panTEAD, rabbit *anti*-FABP4 (Cell Signaling Technologies). Cells were washed twice and then incubated with the corresponding Alexa-conjugated donkey secondary antibodies (ThermoFisher Scientific) for 1 h. Lipid droplets were stained using LipidTox, (ThermoFisher Scientific) and nuclei were counterstained with 4′,6-Diamidino-2-phenylindol (DAPI, Thermo Fisher Scientific).

For cell proliferation analysis, Edu was added to the media at a final concentration of 10 μM. After 24 h (MSCs) or 12 h (CAL51), cells were fixed with paraformaldehyde 4% and stained by Click-iT™ EdU Alexa Fluor™ 647 Imaging Kit (Sigma Aldrich). After the reaction, MSCs were also immunostained with Ki67 antibody (Abcam). Cell were finally counterstained with LipidTox and DAPI.

2.7. Confocal imaging and image quantification

Immunofluorescent stainings were analyzed with Zeiss LSM 780 confocal microscope with either 20× (air) or 40× (oil-immersion) objectives. Z-stacks were acquired with the optimal interval suggested by the software, followed by the application of maximum intensity algorithm.

Lipid accumulation was quantified by measuring with Image J the total positive area for Lipidtox staining, calculated from maximum projections confocal images. The results were divided by the number of DAPI-stained nuclei.

YAP and TEAD nuclear:cytoplasmic ratios were calculated by analyzing with Image J the maximum intensity of the confocal images according to what we previously described [16].

YAP-TEAD-dependent co-transcriptional activity was calculated by dividing mCherry for GFP mean intensities in living reporter cells.

High-resolution confocal image stacks of reporter WT MSCs embedded in fibrin gels were reconstructed by iso-surface rendering using Imaris software v9.0 (Bitplane).

2.8. FACS analysis

Mesenchymal and hematopoietic markers were quantified in undifferentiated MSCs. For this purpose, cells were detached using Tryple express and stained in PBS- BSA 0.2% containing antibody cocktail (CD90-APC, CD34-PE/Cy7, CD105-eFluor 450, CD73^{-}eFluor450, HLA-DR-FITC (ebioscience) CD45-PE, CD14-APC (Biolegend)) for 30 min at 4 °C.

For adipogenesis quantification, cells treated for were cultured for 7 days in adipogenic medium, stained with Lipidtox Deep Red (Thermofisher), washed twice and detached with TrypLE Express (Thermofisher).

The percentage of positive cells was analyzed by BD FACS Canto II and plots prepared using FlowJo software v10 (Tree Star).

2.9. RNA isolation and real-time quantitative PCR analysis

Total RNA was isolated by using the High Pure RNA Isolation Kit according to the manufacturer instructions. One μg of RNA was used to generate the corresponding cDNA with the First Strand cDNA Synthesis Kit (Roche). SYBR Green-based qRT-PCR reactions (LightCycler 480 SYBR Green I Master Kit (Roche)) were run in triplicate in a LightCycler 480 Instrument (Roche). The expression level of individual genes was analyzed by the ΔCt method and normalized according to the expression of the housekeeping gene 18S [28]. Primers sequences are provided in Supplementary Table 3.

2.10. Western blotting

Cells were lysed in RIPA buffer (Merck Millipore) containing 1% protease and phosphatase inhibitor cocktails (Sigma-Aldrich) on ice and then centrifuged at 13.000 g for 10 min at 4 °C. Protein concentration was quantifi3ed by BCA method. 40 μg of proteins per sample were loaded in a 10% polyacrylamide gels (Bio-Rad), pre-run at 40 V for 30 min and then at 100 V until ladder proteins (Bio-Rad) were resolved. Proteins were transferred to a polyvinylidene difluoride membrane using the *Trans*-Blot Turbo transfer system (Bio-Rad). Membranes were blocked with 5% BSA in TBST, incubated with diluted primary antibody in 5% BSA in TBST at 4 °C overnight. The following antibodies were used: rabbit anti-SLUG (9585), rabbit *anti*-E-cadherin (3195), rabbit *anti-N*-cadherin (13116), rabbit *anti*-claudin-1 (13255), rabbit *anti*-ZEB-1 (3396), rabbit *anti*-vimentin (5741) (1:1000, Cell Signaling Technology). After washes, blots were incubated with anti-rabbit IgG, HRP-linked antibody (7074) (Cell Signaling Technology) at RT for 1 h. Chemiluminescence was using Clarity™ Western ECL Substrate (Bio-Rad) and imaged in a ChemiDoc imaging system (Bio-Rad). Mouse *anti*-GAPDH-HRP (Thermo Fisher Scientific) was used as loading control.

2.11. RNA sequencing and data analysis

Libraries were prepared using NEBNext® Ultra™ II Directional RNA

Library Prep Kit for Illumina® with NEBNext® Poly(A) mRNA Magnetic Isolation Module and NEBNext® Multiplex Oligos for Illumina® (Dual Index Primers Set 1). Kits were employed according to manufacturers' protocol, input for library preparation was 200–300 ng total RNA.

Sequencing was done on Illumina NextSeq 500 using NextSeq 500/550 High Output v2 kit (75 cycles). We have done single-end 75 bp sequencing in multiple sequencing runs until all samples had at least 30 million passing filter reads. Fastq files were generated using bcl2fastq software without any trimming.

The quality of the raw sequencing data was assessed using FastQC (https://www.bioinformatics.babraham.ac.uk/projects/fastqc/) and aligned to the hg38 reference genome using the TopHat2 aligner [29]. Raw gene counts were obtained by calculating reads mapping to exons and summarized by genes using reference gene annotation (Ensembl 90; *Homo sapiens* GRCh38. p10, GTF) by HTSeq [30]. Differential gene expression was performed using DESeq2 [31] bioconductor package. Genes were considered as differentially expressed when the Benjamini-Hochberg adjusted *P*-value ≤ 0.05 and log2 fold-change (log2FC) ≥ 1.5. Biological-term classification and the enrichment analysis of gene clusters were performed using clusterProfiler [32]. All computations were performed with R 3.5.1 (R Core Team 2018), and the R packages gplots [33] and GOplot [34] were used.

2.12. Statistical analysis

Unless differently stated, depicted results are expressed as the means ± SEM of at least 3 independent experiments, with more than 5 fields to achieve the count of at least 100 cells for experiments. For singles cell analysis, three technical replicates were performed, and 10 cells per condition were acquired. Differences between groups were compared with Graphpad software using the *t*-test or one-way ANOVA with Holm-Sidak's analysis for multiple comparisons. Two-ways ANOVA followed by Tukey's test analysis were applied to verify the effect of Fibronectin concentration and matrix stiffness. Differences were considered significant when $P < 0.05$.

3. Results

3.1. YAP hinders AD-MSC adipogenic differentiation through its co-transcriptional activity independently of TEAD

The mechano-activated Yes Associated Protein (YAP) has been proposed to control mesenchymal stem cell (MSC) fate by perceiving substrate stiffness. YAP nuclear accumulation occurring when cells are grown onto a stiff surface favors osteogenesis, while it hinders adipogenesis [7].

We asked whether YAP inhibition of adipogenesis requires its transcriptional activity as mediated by the TEAD transcription factor family, which is considered responsible for almost 80% of YAP transcriptional function [15].

We thus generated a stable adipose tissue-derived mesenchymal stem cell (AD-MSC) line expressing nuclear mCherry under the control of 8xTEAD binding sites [35], in order to monitor the activation state of genes directly controlled by YAP-TEAD during adipogenic differentiation.

We exposed transduced AD-MSCs to adipogenic differentiation and monitored live mCherry intensity for one week. A progressive reduction in YAP-TEAD transcriptional activity was detected during adipogenic differentiation, which was not mirrored by cells cultured in growth medium for the same period of time (Fig. 1A, Supplementary Fig. 1A). On a parallel experiment, we co-stained YAP and TEAD in differentiating AD-MSCs and detected a progressive reduction of YAP nuclear presence by immunofluorescence. No change in TEAD localization was found at the same time-points (Fig. 1B). The same results were obtained in non-immortalized primary AD-MSCs (Supplementary Fig. 1B). These results clarified that the reduction observed in YAP-TEAD transcriptional activity during AD-MSC adipogenesis was due to YAP nuclear exclusion and was independent of TEAD localization in the cell.

We then tried to understand whether YAP nuclear exclusion was needed for adipogenesis in AD-MSCs. To this goal, we prompted the differentiation of AD-MSCs transiently transfected with a YAP mutant (YAP-S127A) which cannot be excluded from the nucleus by phosphorylation, thus stably activating its gene program through TEAD [36]. Additionally, we prompted adipogenesis in AD-MSCs transfected with YAP mutant being permanently localized in the nucleus but unable to interact with TEAD (YAP-5SA/S94A) [37]. This mutant activates only the residual 20% of YAP transcription which is independent of TEAD binding. Finally, we repeated the experiment with cells transduced with YAP mutant lacking the PDZ domain (YAP_ΔPDZ), which cannot translocate into the nucleus to activate the transcription [38,39]. Green Fluorescent Protein (GFP) co-transfection was used to identify transduced cells.

The results showed that both transcriptionally active forms of YAP (YAP-S127A and YAP-5SA/S94A) were able to significantly inhibit adipogenic differentiation of AD-MSCs. Instead YAP_ΔPDZ mutant had no effect on adipogenesis. These results confirmed that YAP co-transcriptional activity is needed to hinder adipogenesis. Also, the data suggested a marginal role for TEAD in AD-MSCs commitment towards adipocytes.

To confirm this hypothesis, we induced adipogenesis in AD-MSCs overexpressing two different isoforms of TEAD: TEAD1 and TEAD4. While the overexpression of the former failed in reducing the adipogenic potential of AD-MSCs, the latter had only a limited, although significant effect (Fig. 1C).

This contrasting result prompted us to validate YAP exclusive role in adipogenesis impairment and definitely rule out TEAD participation in the process. Therefore, we enhanced YAP availability for transcription either by: (1) blocking Hippo phosphorylation cascade by MST1/2 inhibitor XMU-MP-1 [40]; or (2) by releasing YAP from TEAD binding through super-TDU, a small molecule designed to physically compete with YAP for TEAD binding site [41].

When adipogenesis was induced, while differing in their ability to activate YAP genetic program through TEAD as quantified by mCherry signal, both small molecules significantly impaired adipogenesis in AD-MSCs, most likely by making YAP more available in the nucleus for TEAD-independent transcription. Collectively, these results showed that YAP availability within the nucleus of AD-MSCs poses an obstacle to adipogenic commitment by activating a genetic program largely independent of TEAD contribution. Therefore, YAP provides the mechanical sensitivity to YAP-TEAD transcriptional complex.

3.2. The depletion of YAP co-transcriptional activity is required for the rearrangement of the cell-ECM interaction and proliferation arrest during adipogenesis

In order to dissect YAP transcriptional program impairing adipogenesis in AD-MSCs, we generated a stable mesenchymal stem cell line overexpressing the transcriptionally hyperactive mutant YAP-5SA, which cannot be phosphorylated and excluded from cell nucleus [42]. First, we confirmed that no change in AD-MSC undifferentiated phenotype was induced by YAP-5SA expression (Supplementary Fig. 2A). Then, by prompting YAP-5SA cell adipogenesis, we demonstrated that the mechanosensitive protein could not be excluded from the nucleus when exposed to adipogenic stimuli, indicating that this phenomenon requires its phosphorylation (Supplementary Fig. 2B). When YAP could not be phosphorylated and excluded from the nucleus, MSCs lost their capacity to commit to adipogenic lineage.

In fact, YAP-5SA AD-MSCs displayed reduced expression of adipocyte markers *ADIPOQ*, *PPARG*, *PLIN1*, failed to acquire FABP4 protein and to accumulate lipid droplets when appropriately stimulated (Fig. 2A, Supplementary Fig. 2C).

Next, we set out to determine which genes are transcriptionally

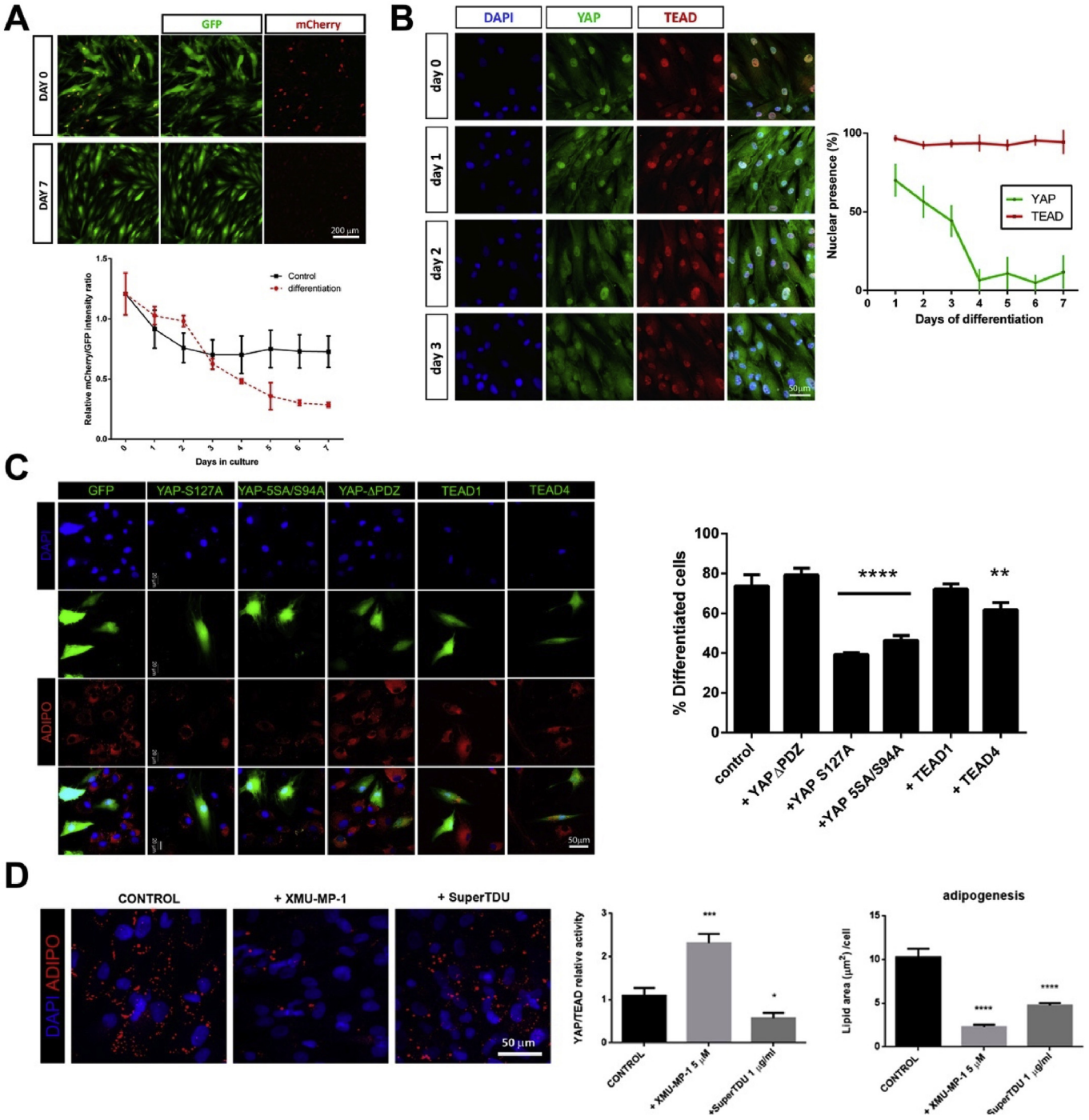

Fig. 1. YAP inhibits adipogenesis through its co-transcriptional activity in a TEAD-independent fashion. A. Top: Representative confocal images of the GFP-positive reporter Mesenchymal Stem Cell (MSC) line with mCherry production being dependent on YAP-TEAD transcription. Bottom: Daily *in vivo* quantification of YAP-TEAD activity during the first week of adipogenic differentiation (red dashed line) as compared to the same cells cultured in growth medium (black line). **B.** Left: Representative immunostaining showing the nuclear presence of YAP and TEAD at the indicated days during adipogenesis. Right: Percentage of MSCs with nuclear YAP or TEAD during the first week of adipogenic differentiation. **C.** Left: Representative confocal fluorescence images of MSCs transfected with plasmids encoding for GFP, alone or in combination with the indicated mutant forms of YAP, TEAD1 and TEAD4, exposed to adipogenic differentiation and stained for lipids (red). Right: Quantification of transfected cells positive for LipidTOX in each indicated condition. **D.** Confocal fluorescence images of MSCs exposed for 3 days to adipogenic stimuli in the presence of MST1/2 inhibitor (XMU-MP-1, 5 mm) or YAP-TEAD inhibitor (SuperTDU, 1 µg/ml) and stained for lipids (red). Nuclei were counterstained with DAPI. Data in the graphs are presented as mean ± SD. ****p-value < 0.0001, ***p-vale < 0.001, **p-value < 0.01, *p-value < 0.05 as obtained by one-way ANOVA followed by Holm-Sidak's tests. (For interpretation of the references to colour in this figure legend, the reader is referred to the Web version of this article.)

altered as a result of YAP-5SA stable expression as compared to the wild type AD-MSCs. By RNA sequencing (RNA-seq) we identified 621 and 696 genes being down- or up-regulated, respectively, by at least 1.5-folds in YAP-5SA cells as compared to the wild type (WT) counterpart (Fig. 2B). The functional annotation of the disregulated genes revealed YAP as a critical modulator of cell-matrix interface (i.e.: cell adhesion, extracellular matrix organization and cell migration) (Fig. 2C). Heat-maps corresponding to the most represented categories can be found in

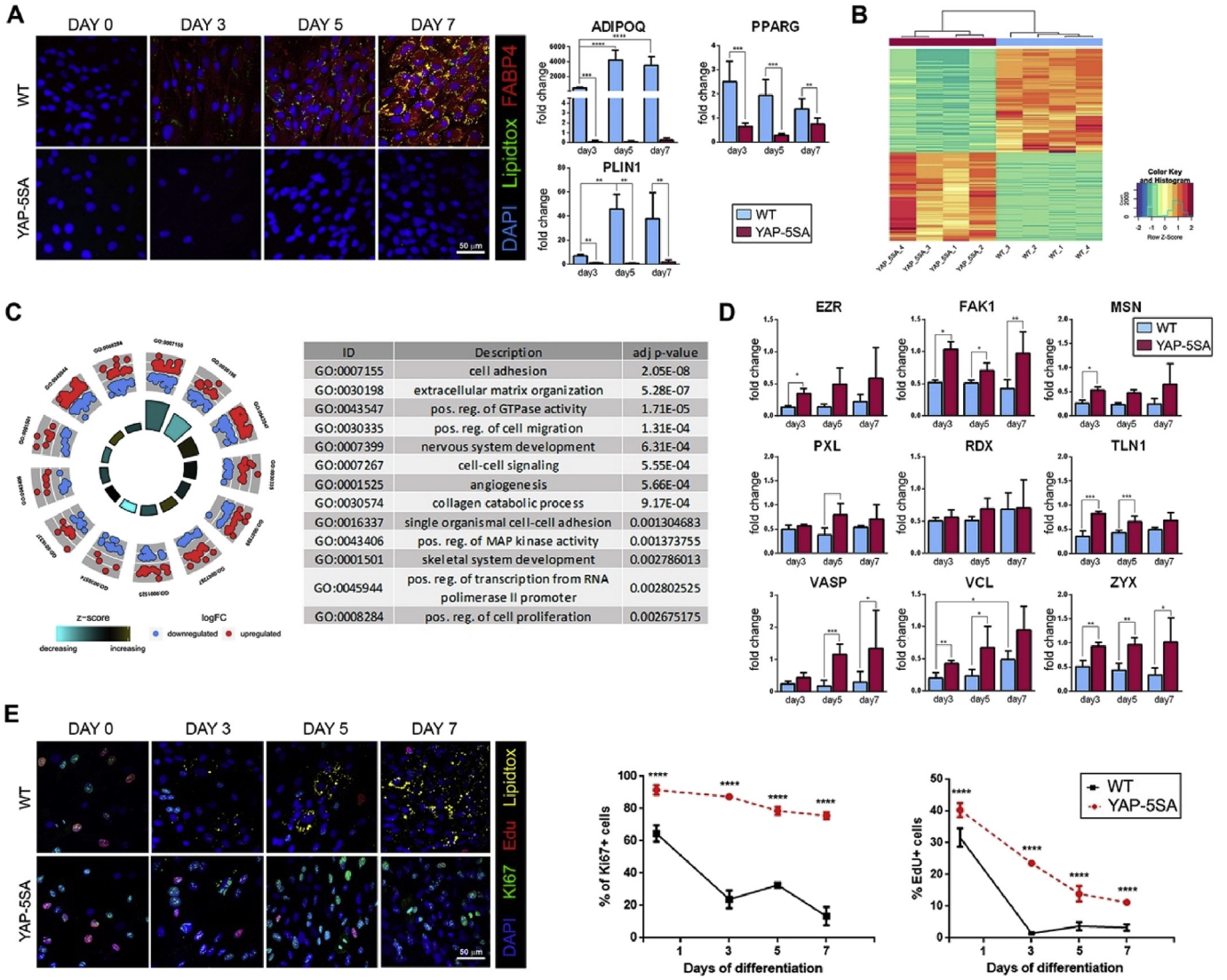

ID	Description	adj p-value
GO:0007155	cell adhesion	2.05E-08
GO:0030198	extracellular matrix organization	5.28E-07
GO:0043547	pos. reg. of GTPase activity	1.71E-05
GO:0030335	pos. reg. of cell migration	1.31E-04
GO:0007399	nervous system development	6.31E-04
GO:0007267	cell-cell signaling	5.55E-04
GO:0001525	angiogenesis	5.66E-04
GO:0030574	collagen catabolic process	9.17E-04
GO:0016337	single organismal cell-cell adhesion	0.001304683
GO:0043406	pos. reg. of MAP kinase activity	0.001373755
GO:0001501	skeletal system development	0.002786013
GO:0045944	pos. reg. of transcription from RNA polimerase II promoter	0.002802525
GO:0008284	pos. reg. of cell proliferation	0.002675175

Fig. 2. YAP nuclear exclusion is required for cell/matrix interface remodeling and cell cycle exit during adipogenesis. A. Left: FABP4 (red) and LipidTOX (green) staining in WT and YAP-5SA MSCs at day 0, day 3, day 5 and day 7 of adipogenic differentiation. Right: qRT-PCR analysis of the adipocyte markers *ADIPOQ*, *PPARG* and *PLIN1* at the indicated time points. **B.** Heatmap showing the clustering of upregulated and downregulated genes in YAP-5SA MSCs as compared to WT MSCs. Four replicates are shown for each category. **C.** Diagram and table showing the 13 most significant gene ontology (GO) categories of genes significantly regulated in YAP-5SA line as compared to WT MSCs. Blue and red dots indicate genes belonging to a given category that are significantly down- or upregulated in YAP-5SA cells, respectively. **D.** qRT-PCR analysis of the expression of the indicated Focal Adhesion-related genes in WT and YAP-5SA MSCs at the indicated timepoints of adipogenic differentiation. **E.** Left: Representative confocal images of WT and YAP-5SA MSCs untreated (day 0) or exposed for 3, 5 and 7 days to adipogenic differentiation medium and stained for Ki67 (green), EdU (red) or lipids (LipidTOX, yellow). Right: quantification of the percentage of Ki67$^+$ and EdU$^+$ cells in WT (black line) and YAP-5SA (red dashed line) at the indicated times of adipogenic differentiation. In all the stainings presented, nuclei were counterstained with DAPI. Graphs represent mean ± SD. ****p-value < 0.0001, ***p-vale < 0.001, **p-value < 0.01, *p-value < 0.05 as obtained by one-way ANOVA followed by Holm-Sidaks statistical analysis. (For interpretation of the references to colour in this figure legend, the reader is referred to the Web version of this article.)

Supplementary Fig. 3. Among the regulated genes, the expression profile of integrin subunits was found altered (*ITGB2*, *ITGA6*, *ITGA7*, *ITGB3*, *ITGA1*, *ITGA9*, *ITGA11*), evidencing the control of YAP over adhesion molecules, in a fashion similar to what previously demonstrated by our group in other cell types [16]. TAZ gene expression was not affected by YAP overexpression.

Focal Adhesion (FA) remodeling is required for MSC adipogenic differentiation [43,44] while the stabilization of adhesion foci - as induced by mechanical stimulation - inhibits adipogenesis [43,45]. Therefore, we quantified by qRT-PCR the expression of a number of key genes encoding for FA- and cytoskeleton-associated proteins in YAP-5SA line under adipogenic stimulation and compared it to the WT line exposed to the same stimuli. Strikingly, the reduction in the expression of several of the genes selected was observed during AD-MSC differentiation. This phenomenon was blunted in YAP-5SA cells exposed to adipogenic stimulation, with *TLN1*, *FAK1*, *VCL*, *VASP* and *ZYX* being significantly regulated as compared to the control at the same time point (Fig. 2D).

Our RNA-seq analysis of the genes differentially regulated in YAP-5SA AD-MSCs also confirmed previous observations indicating that YAP targets genes involved in cell proliferation [15,46]. The regulation of cell cycle is an important event in adipocyte differentiation: during adipogenesis cells undergo limited rounds of proliferation before becoming quiescent [47,48]. Therefore, we monitored the amount of YAP-5SA and WT cells in active phases of cell cycle by staining with Ki67 antibody or proceeding to proliferation by quantifying EdU incorporation during the first week of adipogenic differentiation.

While WT cells lost the proliferation markers promptly after the

adipogenic stimulation started, YAP-5SA cells showed a sustained proliferation in basal conditions. They encountered only a mild reduction in Ki67 during adipogenesis, while the number of cells able to enter S phase was significantly higher than the control at any given timepoint (Fig. 2E). To understand whether cell cycle exit was sufficient for YAP-overexpressing cells to proceed to adipogenesis, we treated YAP-5SA cells undergoing adipogenic stimulation with Mitomycin C. No evidence of differentiation could be detected following Mitomycin treatment of YAP-5SA cells (Supplementary Fig. 4), thus confirming previous results from other groups [9].

These results indicated that the depletion of YAP co-transcriptional activity acts upstream of FA-cytoskeleton rearrangement and proliferation arrest in AD-MSCs induced to adipogenesis. Since cell cycle exit in the presence of nuclear YAP was not able to restore adipogenesis (Supplementary Fig. 4), we focused on the interplay between cell adhesion and YAP in controlling adipogenesis.

3.3. Cell spreading modulates AD-MSC adipogenic differentiation by controlling YAP nuclear localization independently of focal adhesion formation

The chemical inhibition of FA formation has been shown to increase MSC adipogenic differentiation [49,50]. Given the predominant annotation for cell adhesion genes found by RNA-seq in YAP-5SA line and the inability of such cell line to proceed to adipogenic commitment, we decided to decouple the role of cell adhesion and YAP mechanosensing during adipogenesis.

Therefore, we seeded AD-MSCs on substrates coated with Poly-L-Lysine (PLL), and confirmed that they displayed impaired FAs and reduced cell spreading. These cells also exhibited low nuclear YAP presence (Fig. 3A). As expected, when appropriately stimulated, cells on PLL acquired the adipogenic features more promptly than on TCPS (Fig. 3B).

A limited reduction in YAP presence was also induced by PLL in YAP-5SA cells, thus indicating that this event mostly depends on YAP phosphorylation. These cells continuously formed FAs even when stimulated with adipogenic medium and failed to accumulate lipid droplets (Fig. 3B). The stabilization of FAs via manganese (Mn^{2+}) integrin activation [51,52] reduced the adipogenic potential in WT cells and had no effect on YAP-5SA cell phenotype (Supplementary Fig. 5).

In order to discriminate between the contribution to adipogenesis of FAs remodeling and YAP nuclear presence as determined by cell spreading, we designed fibronectin-coated micropatterned surfaces suited for single-cell culture, allowing to keep a constant cell spreading area (4900 μm^2), while reducing the adhesion surface (4900 μm^2, 1000 μm^2, 450 μm^2 or 254 μm^2) [16].

The reduction of the adhesion area caused a steady decrease in total FA area, as quantified by vinculin-rich spikes. Interestingly, when the adhesion area was reduced below the total area of FA formed in unrestricted conditions (458,5 ± 62,68 μm^2), cells became unable to induce the assembly of FAs and vinculin appeared completely cytoplasmic (Fig. 3C).

Despite the changes observed in FAs due to the reduction of adhesion site availability, YAP nuclear presence remained unaltered in all the adhesion areas studied.

We then exposed these cells to adipogenic stimulation and monitored the appearance of lipid droplets after 3 days (Fig. 3D). Only WT AD-MSCs which did not spread completely and displayed a reduced YAP expression exhibited lipid staining.

Overall, these data compellingly indicate that cell spreading restricts AD-MSC adipogenic potential by controlling YAP nuclear presence and co-transcriptional activity, independently of FA formation.

3.4. F-actin stability mechanically controls AD-MSC adipogenic potential through YAP nuclear exclusion independently of its phosphorylation

As previously demonstrated by our group and others, YAP nuclear translocation is controlled by the transmission of tension through the cell cytoskeleton [18,19,53]. Cell tension, resulting from the contribution of F-actin stability and Myosin II activity, has been shown to control hMSC fate [9]. Also, selective inhibitors of F-actin polymerization and of Myosin II activity were proven to trigger YAP cytoplasmic accumulation [48]. No causal correlation between cytoskeleton tension and adipogenesis through YAP has been so far established.

Therefore, we seeded AD-MSCs at a density which would favour adipogenesis without inducing YAP cytoplasmic shuttling through cell-cell interaction, and stimulated them with adipogenic supplements in the presence of increasing concentrations of either F-actin disruptor cytochalasin D or the inhibitor of the ATPase activity of Myosin II, blebbistatin.

In this experimental setting, we confirmed that both tension inhibitors were able to exclude YAP from the nucleus of WT AD-MSCs in a dose-dependent fashion (Fig. 4A). As expected, YAP exclusion was accompanied by a concomitant, concentration-dependent, increase in adipogenesis. On the other hand, only F-actin inhibitor was able to partially exclude YAP from the nucleus of YAP-5SA cells, as shown by YAP nuclear/cytoplasmic ratio, and restore adipogenesis in YAP-5SA AD-MSCs when appropriately stimulated. Such effect was not phenocopied by treating the cells with Myosin II inhibitor blebbistatin (Fig. 4A and B).

Cytoskeleton tension can be finely tuned by confining single cells on fibronectin-coated micropatterned surfaces of defined areas ranging from 300 to 10000 μm^2 [7,16,18]. Confined cells having a reduced cytoskeleton tension display YAP cytoplasmic accumulation [7]; the same culture condition was proven to prompt adipogenic differentiation as compared to spread cells [9].

We confirmed that in single micropatterned AD-MSCs exposed to adipogenic stimulation, the ability to accumulate lipid droplets inversely correlated with cell area, tension and YAP nuclear localization: smaller cells having a lower YAP nuclear:cytoplasmic ratio as a result of reduced tension, were more prone to differentiate as compared to bigger cells with a higher cytoskeleton tension and YAP ratio (Fig. 4C). A similar correlation between cell area, nuclear YAP and adipogenic differentiation was obtained in primary non-immortalized AD-MSCs (Supplementary Fig. 6). In fact, lipid accumulation was not significantly different in cells seeded onto micropatterns with constant surface area but with different circularity index and inducing no changes in YAP nuclear presence (Supplementary Fig. 7A).

On the contrary, micropatterned YAP-5SA cells showed a sustained nuclear presence of the protein when the area was ranging from 1024 μm^2 to 10000 μm^2, while YAP nuclear:cytoplasmic ratio was slightly reduced on 300 μm^2 as compared to 10000 μm^2 islands, but still comparable to 1024 and 2025 μm^2. The amount of nuclear YAP in YAP-5SA cells grown onto 300 μm^2 was still sufficient to impair adipogenesis. In fact, none of the cells analyzed could accumulate lipids in the presence of appropriate biological supplements (Fig. 4C).

In the conditions tested, cell spreading did not affect TEAD localization (Fig. 4D), thus arguing against the possibility that the transcription factor could be mechanoregulated per se, likely previously suggested elsewhere [54]. TEAD also remained nuclear after adipogenic induction regardless of cell area (Supplementary Fig. 7B).

Altogether, these data demonstrate that the mechanical regulation of AD-MSC adipogenesis occurs as the result of two regulatory systems: one mediated by cytoskeletal integrity, which is independent of YAP phosphorylation, and another pathway dependent on myosin II cell tension, which relies on the phosphoregulation of the Hippo effector.

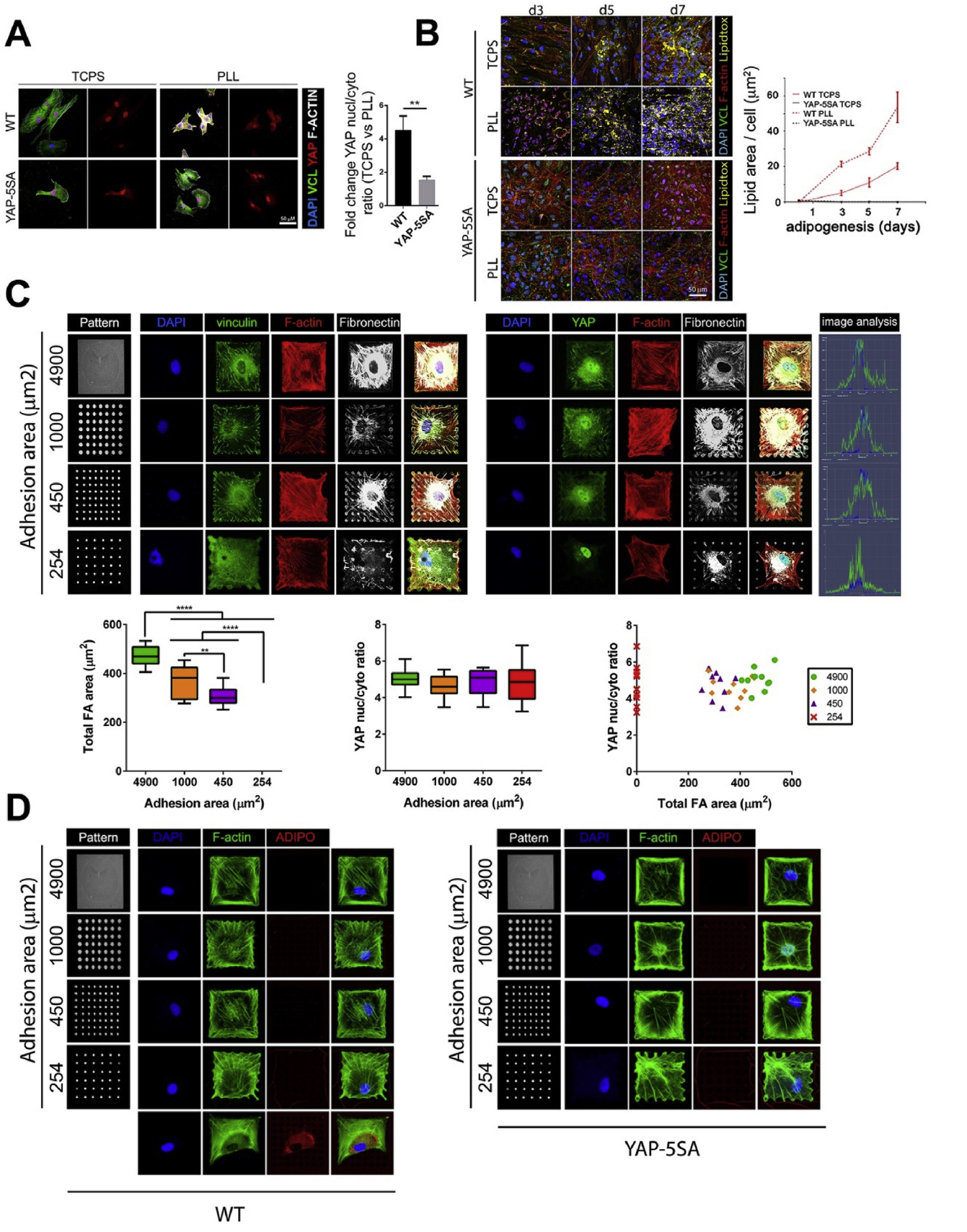

(caption on next page)

Fig. 3. Cell spreading controls adipogenesis by regulating YAP nuclear presence regardless of adhesion area. A. Representative confocal images of WT and YAP-5SA MSCs seeded on tissue culture polystyrene (TCPS) or Poly-L-lysine (PLL)-coated surfaces and stained for YAP (red), vinculin (VCL, green), F-actin (white) and DAPI (blue). The bargraph shows the comparison between YAP nuclear/cytoplasmic ratio in MSCs cultured on PLL-coated- as compared to the same cells grown on non-coated TCPS. The values are indicated as fold changes. **B.** Left: Representative confocal images of WT and YAP-5SA MSCs cultured on tissue culture polystyrene (TCPS) or Poly-L-lysine (PLL)-coated surfaces in adipogenic medium for the indicated days and stained for vinculin (VCL, green), F-actin (red), lipids (LipidTOX, yellow) and counterstained with DAPI (blue). Right: quantification of lipid area per cell as obtained at the indicated timepoints and conditions. **C.** Representative confocal images of single WT MSCs cultured onto micropatterns having constant spreading area (4900 μm^2) and the indicated adhesion areas. Cells were stained for vinculin (green, left) and YAP (green, right). In both panels cells were stained for fibronectin (white), F-actin (red) and DAPI (blue). Down: Boxplot representing the median ± min/max of total focal adhesion area (left), YAP nuclear/cytoplasmic ratio (center) and dotplot representing the distribution of the indicated parameters (right) in a subset of 10 cells having the reported adhesion area. **D.** Representative confocal images of WT and YAP-5SA MSCs cultured onto micropatterns having constant spreading area (4900 μm^2) and the indicated adhesion areas, induced to adipogenic differentiation for 3 days and stained for F-actin (green), lipids (LipidTOX, red) and counterstained with DAPI (blue). ****p-value < 0.0001, **p-value < 0.01 as calculated by one-way ANOVA followed by Holm-Sidak's tests. (For interpretation of the references to colour in this figure legend, the reader is referred to the Web version of this article.)

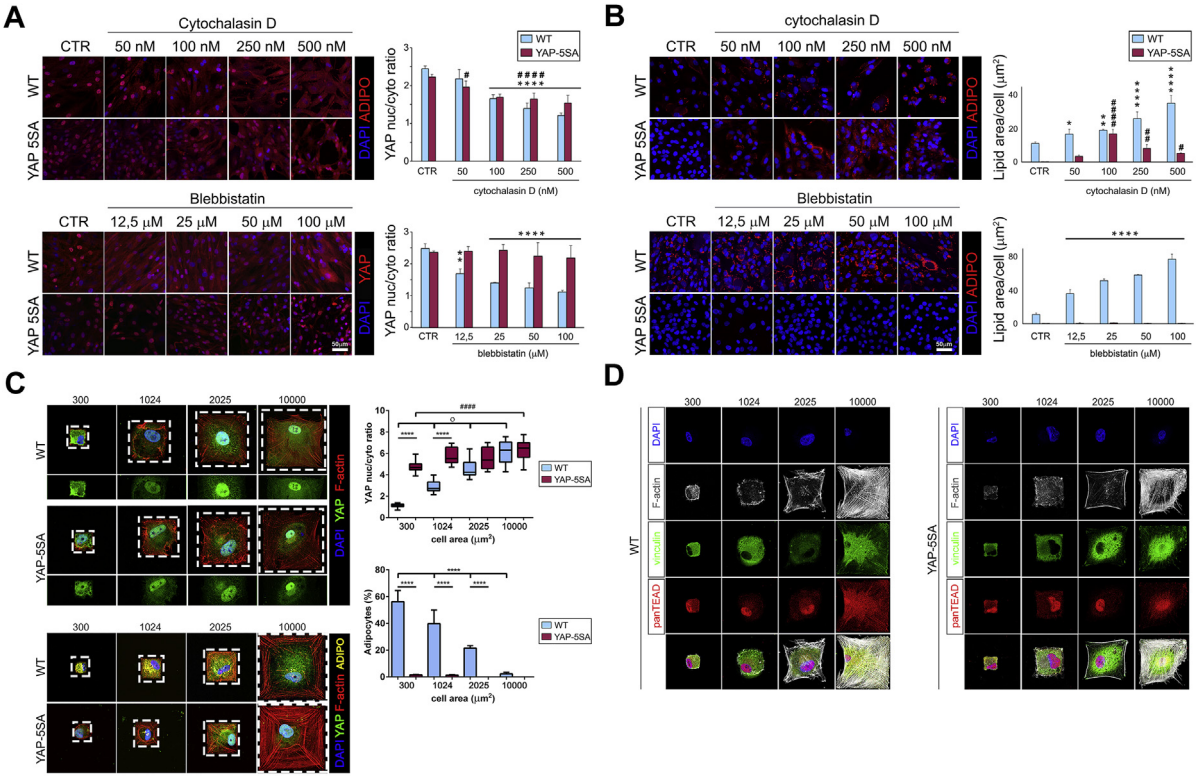

Fig. 4. The mechanical regulation of adipogenesis by cell spreading is mediated by YAP in a Filamentous Actin/YAP-phosphorylation independent and Myosin II/Phospho-YAP-dependent manner. A. Representative confocal images of YAP staining in WT and YAP-5SA MSCs treated with the F-actin disruptor Cytochalasin D (up) and Blebbistatin (down) at the indicated concentrations for 24 h. Graphs: quantification of YAP nuclear/cytoplasmic ratio in WT and YAP-5SA cells treated with F-actin inhibitors. **B.** Representative confocal images of lipid staining by LipidTOX (red) in WT and YAP-5SA MSCs grown in adipogenic media for 72 h and treated with Cytochalasin D (up) and Blebbistatin (down) at the indicated concentrations. Graphs: corresponding quantification of the lipid area/cell. Bars represent mean ± SD. Asterisks represent the p-value obtained by comparing WT cells and the respective untreated control, while hashtags indicate the value obtained by comparing WT cells against the untreated YAP-5SA. **C.** Up: Representative confocal images of single WT and YAP-5SA MSCs grown onto fibronectin-coated micropatterns having the indicated adhesion area stained for YAP (green) and F-actin (red). Dashed lines indicate the adhesion area and the inset highlights YAP intracellular localization. Graph: quantification of the YAP nuclear/cytoplasmic ratio for WT (blue) and YAP-5SA (purple) cells of a given area. Values are shown as median ± min/max. Down: Representative confocal images of single WT and YAP-5SA MSCs grown onto micropatterns with increasing surface area for 3 days in adipogenic medium and stained for YAP (green), F-actin (red), and lipids (LipidTOX, yellow). Graph: Quantification of cells positive for lipid staining for each condition studied. Bars represent mean ± SD ****p-value < 0.0001, *p-value < 0.05. **D.** Representative confocal images of single WT and YAP-5SA MSCs grown onto fibronectin-coated micropatterns having the indicated adhesion area and stained for TEAD (red), vinculin (green) and F-actin (white). **** or #### p-value < 0.0001, ** or ## p-value < 0.01, * or # p-value < 0.05 as calculated by one-way ANOVA followed by Holm-Sidak's tests. In all the presented pictures nuclei were counterstained with DAPI (blue). (For interpretation of the references to colour in this figure legend, the reader is referred to the Web version of this article.)

3.5. Dimensionality dictates substrate mechanics effects on adipogenesis by controlling YAP phosphorylation through cell spreading

A recent report indicated YAP localization displaying divergent dependency on substrate stiffness in 2D and 3D culture conditions [55]. This study considered YAP response to substrate stiffness in terms of protein localization, but did not connect matrix mechanics to YAP actual transcriptional activity nor proved its effect on differentiation.

We cultured our mCherry-based YAP-TEAD AD-MSC mechano-reporter line onto or within fibrin hydrogels with controlled stiffness. Also, we combined our YAP-5SA AD-MSC line with mCherry YAP-TEAD mechano-reporter system and used this new cell line in the following experiments.

Hydrogels of different stiffnesses were obtained by mixing different proportions of thrombin and fibrinogen according to previously published data [27], in order to produce compliant (300 Pa) and stiff (5 kPa) hydrogels able to differentially control YAP nuclear localization [56]. To avoid the degradation of the hydrogels, which would hinder

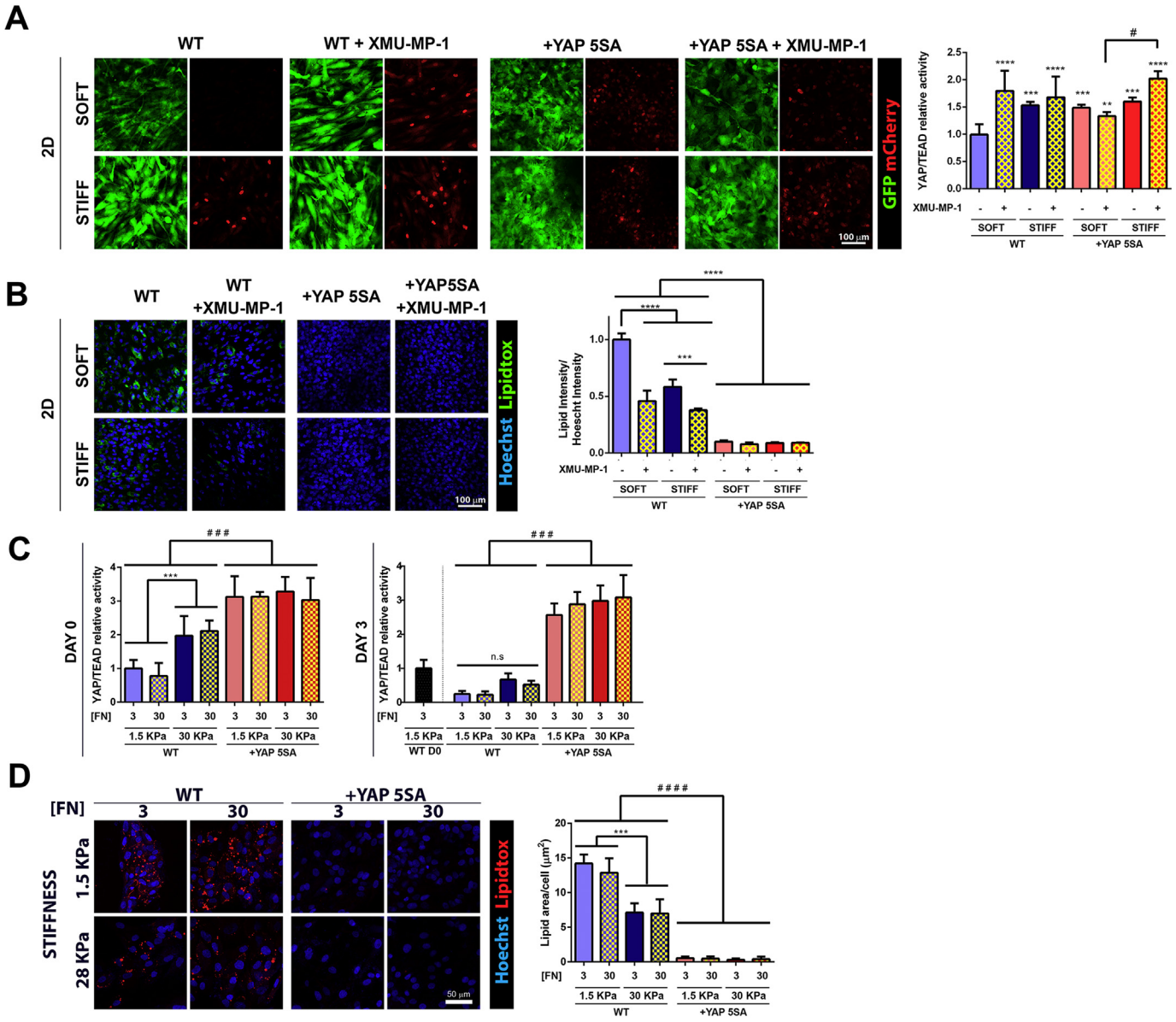

Fig. 5. 2D cell spreading is determined by substrate stiffness and controls adipogenesis through YAP phosphorylation. A. Representative confocal images of WT and YAP-5SA MSCs mechano-reporter cell lines seeded onto soft (300 Pa) or stiff (5 kPa) fibrin hydrogels, treated or not with the MST1/2 inhibitor XMU-MP-1 (left). Right: relative quantification of YAP-TEAD transcriptional activity, as measured by mCherry/GFP fluorescence intensity. Asterisks over the bars represent the p-value significance for values obtained in WT and YAP-5SA cells as compared to WT cells grown onto soft hydrogel, while hashtags correspond to the comparison between YAP-5SA cells treated with XMU-MP-1 in soft and stiff hydrogel. **B.** Representative confocal images and quantification of WT and YAP-5SA cells grown onto soft and stiff hydrogels, treated or not with XMU-MP-1 and stained for lipids (LipidTOX, green) and nuclei (Hoechst, blue) after 3 days exposure to adipogenic medium. Bars represent mean ± SD. ****p-value < 0.0001, ***p-vale < 0.001, ** or $^{\#\#}$ p-value < 0.01, * or $^{\#}$ p-value < 0.05, as obtained by one-way ANOVA test followed by Holm-Sidak's multiple comparison test. **C.** Quantification of YAP-TEAD activity in WT and YAP-5SA mechanoreporter MSCs seeded onto PDMS dishes with stiffnesses ranging from 1.5 to 28 KPa, coated with 3 or 30 µg/ml fibronectin, before differentiation (left graph, day 0) and 3 days after being exposed to adipogenic cocktail (right graph, day 3). **D.** Representative confocal images and quantification of WT and YAP-5SA cells grown onto PDMS substrates, stained for lipids (LipidTOX, red) and nuclei (Hoechst, blue) after 3 days exposure to adipogenic medium. Bars represent mean ± SD. *** or #### p-value < 0.001, #### p-value < 0.0001. Hagstags correspond to the p-values calculated by two-ways ANOVA comparison between stiffness and ligand density, while asterisks correspond to the post-hoc Tukey's multiple comparison. (For interpretation of the references to colour in this figure legend, the reader is referred to the Web version of this article.)

the nature of the experiment, aprotinin was added to the mixture [57].

As expected, cells cultured onto 2D stiff (5 kPa) hydrogels could spread better as compared to cells growing onto soft (300 Pa) surfaces.

As a consequence, a significant difference in YAP-TEAD transcriptional activity was found among cells grown onto stiff vs. soft 2D substrates, as quantified by mCherry intensity (Fig. 5A). Instead, no difference in the transcriptional activity could be found when YAP-5SA cells were cultured onto soft or onto stiff hydrogels. This result once again suggests that substrate mechanics regulates YAP transcriptional activity by phosphorylation. As a control, cells cultured in the presence of MST1/2 inhibitor XMU-MP-1 showed enhanced YAP-TEAD transcriptional activity regardless of matrix stiffness.

When the cells grown onto the hydrogels were exposed to adipogenic stimulation, we found that the lipid accumulation correlated inversely with YAP-TEAD transcriptional activity: cells grown onto soft substrate had an enhanced adipogenic commitment as compared to MSCs in stiffer gels, and adipogenesis was prevented by the expression of hyperactive YAP (YAP-5SA) and by MST1/2 kinase activity

inhibition (Fig. 5B).

Since fibrinogen concentration modifies gel stiffness but can also change ligand density [58], we decided to decouple both effects by using PDMS plates with stiffness ranging from 1.5 kPa to 28 KPa and coated with 2 different concentrations of fibronectin (3 and 30 μg/ml). While confirming the effect of substrate stiffness on adipogenesis through YAP (Supplementary Fig. 8), this experiment showed no effect of ligand density in the range of fibronectin studied over YAP activity (Fig. 5C left). Adipogenic stimulation caused a significant drop in YAP-TEAD reporter activity in WT cells, independently of substrate stiffness or fibronectin concentration (Fig. 5C right), demonstrating that YAP-TEAD activity at the moment of the adipogenic stimulation determines the success of the initiated program.

As predicted, again substrate stiffness correlated inversely with lipid droplet accumulation, this effect being independently of the fibronectin concentration (Fig. 5D). Consistently, the overexpression of YAP-5SA fueled YAP-TEAD transcriptional activity and abolished adipogenic commitment regardless of substrate stiffness and fibronectin concentration.

Then, we asked whether a similar interplay among substrate stiffness, YAP-TEAD transcriptional activity and adipogenesis could be found in 3D hydrogels. We embedded YAP-TEAD AD-MSCs mechano-reporter cells in 3D fibrin hydrogels having the same stiffness values observed in 2D and quantified mCherry intensity. Soft 3D hydrogels, which allowed cell spreading, prompted YAP-TEAD transcriptional activity. On the contrary, stiff 3D hydrogels prevented cell spreading, kept them in a rounded morphology and reduced mCherry intensity (Fig. 6A, Supplementary Video 1 and 2). Releasing MST1/2 inhibition by XMU-MP-1 abolished stiff substrate effect and restored YAP-TEAD transcriptional activity. As expected, the impossibility to phosphorylate YAP in YAP-5SA cells prevented 3D substrate stiffness effect (Fig. 6B).

Supplementary video related to this article can be found at https://doi.org/10.1016/j.biomaterials.2019.03.009.

Consistent with the hypothesis that YAP nuclear function impairs adipogenesis, cells exposed to adipogenic stimulation within stiff matrices were more prone to differentiate as compared to those embedded into soft hydrogels. In this context, XMU-MP-1 treatment or the presence of hyperactive YAP-5SA mutant had similar effects and inhibited adipogenesis (Fig. 6C).

In order to decouple the effects of ligand density and 3D stiffness on YAP activity and differentiation, we embedded cells in commercially available PEG-based hydrogels with different stiffnesses (soft: ~300 Pa, stiff: ~1500 Pa) and functionalized to obtain the same ligand density. Cells embedded in the soft material showed a significantly higher apparent area when compared to cells growing in the stiff PEG hydrogels.

Again, a consistent difference in YAP-TEAD transcriptional activity was observed in WT cells and correlated with a differential ability to proceed to adipogenic commitment (Fig. 6D). On the contrary, when we seeded the cells in PEG-based hydrogels with same stiffness but different ligand density, no significant changes were observed either in YAP-TEAD activity or adipogenic commitment (Fig. 6F). As expected, YAP-5SA cells showed no difference in YAP-TEAD activity and no adipogenic commitment was observed in any condition tested.

These results collectively and compellingly demonstrate that YAP transcriptional activity, as determined by cell ability to spread over or within a permissive environment, impairs mesenchymal stem cell adipogenic differentiation.

3.6. Cancer-to-adipocyte reprogramming can be enhanced by targeting YAP activity

A recent report described a methodology to reduce cancer cell growth and invasiveness by promoting their epithelial-to-mesenchymal (EMT) transition and then reprogramming them into non-proliferative adipocyte-like cells [26]. Given the acknowledged role of YAP as oncogene [38,59] and our observations that it acts as an inhibitor of adipogenic commitment, we decided to investigate whether - by mechanically modulating YAP activity - we could induce adipogenic transdifferentiation in a model of breast cancer. The experimental design is depicted in Fig. 7A.

We knocked out YAP in breast cancer cell line CAL51 by CRISPR/Cas9 technology [16]. The analysis of proteins related to EMT showed that YAP-depleted cells lost the expression of epithelial-related proteins such as E-cadherin or Claudin-1, while acquired some proteins related to the mesenchymal phenotype such as SLUG, TCF-8/ZEB1, Vimentin and N-cadherin (Fig. 7B).

When the cells were exposed to adipogenic medium, $YAP^{-/-}$ cancer cells accumulated lipid droplets (Fig. 7C), which also correlated with the *de novo* expression of the adipogenic marker *PLIN2* (Fig. 7D). Adipogenic stimulation also reduced $YAP^{-/-}$ CAL51 proliferation by ≈ 50% (Fig. 7E). No adipogenic commitment and a milder inhibition of the proliferation were detected in wild type cells expressing YAP.

In order to check whether the mechanical control of YAP-TEAD transcriptional activity in CAL51 tumor cells could trigger their adipogenic reprogramming, we embedded WT and $YAP^{-/-}$ CAL51 cells in the fibrin hydrogels with controlled stiffness described above. CAL51 mechano-reporter cell line confirmed the mechanical control over YAP-TEAD transcriptional activity so that it was higher in soft fibrin gels, where the cells could spread better (Fig. 7F). When exposed to adipogenic medium, the accumulation of lipid droplets in WT CAL51 cells was only induced on the less compliant environment, as a result of the restriction of YAP-TEAD transcriptional activity. On the contrary, $YAP^{-/-}$ CAL51 cells accumulated lipid droplets independently of the stiffness of the hydrogel (Fig. 7G).

Collectively, these results indicate materials control over YAP expression and YAP-TEAD transcriptional activity as a tool to possibly decrease tumor proliferation and spreading by promoting their conversion in postmitotic adipocyte-like cells.

4. Discussion

The implantation of mesenchymal stem cells (MSCs) has been proposed for a number of regenerative medicine applications, due to their potential to generate functional somatic cells of the mesodermal lineage (i.e.: osteoblasts, adipocytes, chondrocytes). Besides being an advantage for their versatility, MSC plasticity poses the issue of the control of their phenotype, in order to avoid that they drift to differentiate towards unwanted cell types when implanted *in vivo*. While prompting MSC adipogenesis might be beneficial in cases when lipofilling is required after cancer surgery [25], in bone regeneration applications, fat formation is considered a side effect. The tight control of adipogenesis could potentially overcome the accumulation of visceral fat observed in normal organs and that reduces their functionality during aging [60].

Mesenchymal stem cell fate can be controlled by substrate mechanical cues [2], as sensed and propagated through the cell cytoskeleton [9]. The transmission of mechanical cues inward to the nucleus directly controls cell function by dictating gene expression [7].

Therefore, the use of biomaterials to tightly regulate implanted MSC fate paves the way to the setup of innovative materials-based clinical applications.

The mechanosensing role of Yes Associated Protein (YAP) and WW domain-containing transcription regulator protein 1 (WWTR1 or TAZ) has been lately elucidated by showing their ability to dynamically interpret modifications in microenvironment compliance and shuttle to the cell nucleus [18].

Most of previous studies have only established a correlation between two coincident phenomena following alterations in ECM mechanics: changes in YAP nuclear localization and co-transcriptional activity were associated with a switch in MSC commitment [6,61,62].

Functional experiments only lately confirmed that silencing of YAP or its paralog protein TAZ hinders the effect of matrix stiffness [7], flow stress [17], or spreading [7,16] on MSC adipogenic/osteogenic switch.

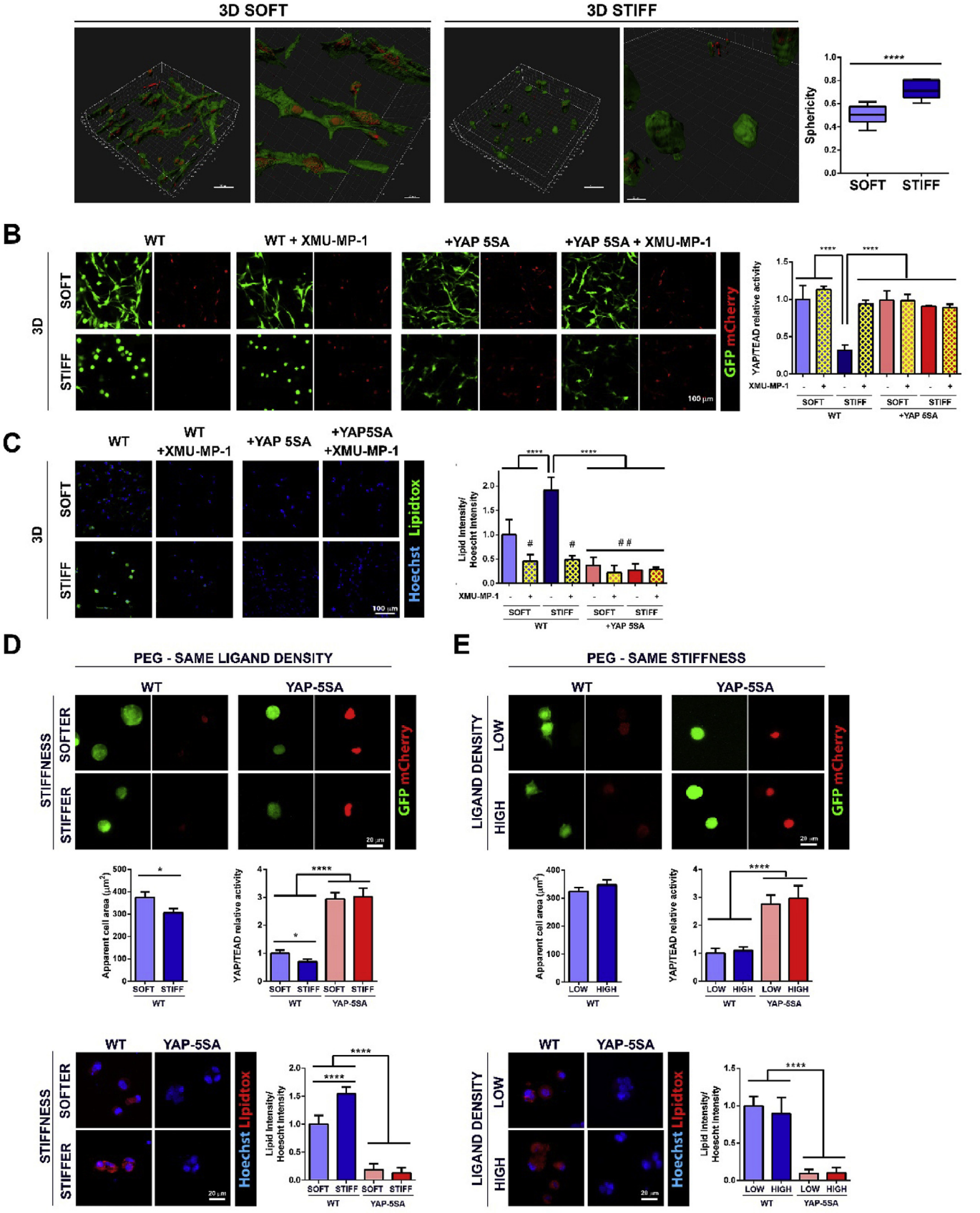

(caption on next page)

Fig. 6. Substrate stiffness controls adipogenesis through YAP phosphorylation regulation by determining cell spreading in a 3D environment. A. Isosurface rendering by IMARIS software of confocal z-stacks obtained from WT MSCs mechano-reporter cell lines embedded in soft (300 Pa) or stiff (5 kPa) fibrin hydrogels. Graph: Quantification of WT cell sphericity in 3D soft or stiff fibrin hydrogels. The boxplot represents median ± min/max ****p-value < 0.0001, *t*-test. **B.** Representative confocal images of WT and YAP-5SA MSCs mechano-reporter cell lines embedded in soft (300 Pa) or stiff (5 kPa) fibrin hydrogels (left), treated or not with XMU-MP-1 (left) and relative quantification of YAP-TEAD transcriptional activity by mCherry/GFP fluorescence intensity. **C.** Representative confocal images of WT and YAP-5SA cells grown into 3D soft and stiff hydrogels, treated or not with XMU-MP-1 and stained for lipids (LipidTOX, green) and nuclei (Hoechst, blue) after 3 days exposure to adipogenic medium. Hashtags over the bars represent the p-value significance when compared to WT cells embedded in soft hydrogels. Data presented in the figure were normalized to the value of WT cells in soft hydrogels. Bars represent mean ± SD. ****p-value < 0.0001, ***p-vale < 0.001, ** or $^{\#\#}$ p-value < 0.01, * or $^{\#}$ p-value < 0.05, as obtained by one-way ANOVA test followed by Holm-Sidak's multiple comparison test. **D.** Top: Representative confocal images of WT and YAP-5SA MSCs mechano-reporter cell lines embedded in soft (300 Pa) or stiff (1500 Pa) PEG hydrogels functionalized to have the same ligand density. Center: Quantification of apparent cell area of WT cells grown in both PEG hydrogels (*p-value < 0.05, *t*-test) and relative quantification of YAP-TEAD transcriptional activity by mCherry/GFP fluorescence intensity. Bottom: Representative confocal images of WT and YAP-5SA cells embedded in soft or stiff PEG hydrogels and stained for lipids (LipidTOX, red) and nuclei (Hoechst, blue) after 3 days exposure to adipogenic medium. **E.** Top: Representative confocal images of WT and YAP-5SA MSCs mechano-reporter cell lines embedded in PEG hydrogels with the same stiffness but functionalized to have different ligand density (low, high). Center: Quantification of apparent cell area of WT cells grown in PEG hydrogels (p-value > 0.05 *t*-test) and relative quantification of YAP-TEAD transcriptional activity by mCherry/GFP fluorescence intensity. Bottom: Representative confocal images of WT and YAP-5SA cells embedded into soft and stiff PEG hydrogels and stained for lipids (LipidTOX, red) and nuclei (Hoechst, blue) after 3 days exposure to adipogenic medium. Bars represent mean ± SD. ****p-value < 0.0001, or *p-value < 0.05, as obtained by one-way ANOVA test followed by Holm-Sidak's multiple comparison test. (For interpretation of the references to colour in this figure legend, the reader is referred to the Web version of this article.)

Thus, the question whether substrate mechanics favours one given phenotype by regulating YAP/TAZ protein shuttling and turnover is still to be answered.

Here we adopted a number of distinct bioengineering tools based on single cell patterning, 2D and 3D hydrogels with controlled mechanics in the physiological range (0.3, 5 kPa) and ligand density in order to decouple the role of mechanical and biological signals on adipogenesis. We compellingly demonstrate that the mechanical control of YAP shuttling to the nucleus and its co-transcriptional activity, independently of TEAD binding, is of paramount importance for MSCs to proceed towards the adipogenic phenotype. Moreover, starting from the recent evidence that tumor cell proliferation and spreading can be arrested by prompting their adipogenic transdifferentiation [26], we provide evidence that YAP activity can be mechanically controlled in breast cancer cells to halt their proliferation and induce the formation of harmless adipose cells.

4.1. The mechanical regulation of MSC fate relies on cell spreading controlling YAP co-transcriptional activity

Starting from the indication that adipogenesis can be induced in MSCs by biological stimulation and favoured by either a soft microenvironment or by cell confinement [7,9], we provide evidence that MSC adipogenic fate is ruled by cell inability to spread in a non-permissive environment. These results are supported by our experiments entailing the confinement of single MSCs onto 2D micropatterned areas, confirming what previously demonstrated [9].

More importantly, they are corroborated by imposing constraints to cell spreading in 2D and 3D hydrogels, in the presence of the same biological stimuli and chemical composition. In fact, conditions preventing cell spreading regardless of the dimensionality favour MSC adipogenesis. Interestingly, while cells grown onto a 2D hydrogel need a soft matrix to become adipocytes, the acquisition of such phenotype in 3D requires a stiff environment.

The differences in YAP behaviour in 2D versus 3D could partially explain the discrepancies between the *in vitro* and *in vivo* results [63], making harder the translation of experimental achievements obtained by reductionist bi-dimensional experiments into a clinical setting.

In our previous study, we correlated YAP subcellular localization with the ability of the cell to spread and inversely associated Hippo effector activation with adipogenesis [16].

Here we further the notion that YAP localization is regulated downstream of cell area, and for the first time establish that cell spreading, as determined by substrate mechanics, controls YAP co-transcriptional activity, which, in turn, negatively regulates adipogenesis.

In our experimental setup, we also ruled out the possibility that the effects of ligand density are hidden behind substrate stiffness. Indeed, functionalized PEG hydrogels and PDMS substrates with controlled stiffness and ligand density compellingly clarify that substrate compliance determines MSC ability to commit to the adipogenic phenotype by controlling YAP co-transcriptional activity. Both our 2D and 3D experiments point at cell ability to spread and subsequently generate intracellular tension in a permissive environment as key determinants in YAP control over MSC commitment. Unfortunately, these data do not allow us to decouple cell spreading from tension, like previously shown in a more dynamic setting [64].

Recently, the group of Mooney suggested that 3D viscoelastic hydrogels having controlled force relaxation mimic better native ECM response to cell force and show no direct dependence of MSC commitment from YAP nuclear localization [65]. Here we adopted purely elastic (PEG) and partially viscoelastic (fibrin) hydrogels and measured how YAP co-transcriptional activity – rather than its mere subcellular localization - is mechanically regulated.

If put in perspective with previous studies, our original data suggest that adipogenesis might be regulated in a more complex fashion by ECM mechanics and viscoelasticity *in vivo*, rather than being simply based on the binary regulation of YAP shuttling.

Nonetheless, the reductionist model for cell mechanosensing we adopted allowed us to determine that the mechanical regulation of MSC adipogenesis requires YAP nuclear exclusion through phosphorylation. In fact, adipogenesis was prevented by expressing in MSCs the nuclear non-phosphorable YAP mutant (YAP-5SA) or by treating the same cells with pharmacological inhibitor of upstream kinase cascade (XMU-MP-1). These results were confirmed regardless of the dimensionality, independently of the adipogenic stimulation being applied to MSCs.

The ability of cells to spread in a permissive environment requires the correct propagation of internal mechanical forces, as controlled by cytoskeleton tension being produced by the interplay of filamentous actin and motor protein Myosin II [66].

By studying the behaviour of the non-phosphorable mutant of YAP, we concluded that the regulation of adipogenesis by substrate mechanics occurs through YAP and needs the concomitant activity of two axes: the first one relies on the tension generated by myosin II motor and impacts on the Hippo phosphorylation cascade. The second system is based on the integrity of actin cytoskeleton itself and is phosphorylation-independent.

Since the contribution of the two-tension axes to the control of adipogenesis through YAP may depend on the range of force applied, combined effects are to be expected to act in a physiological environment.

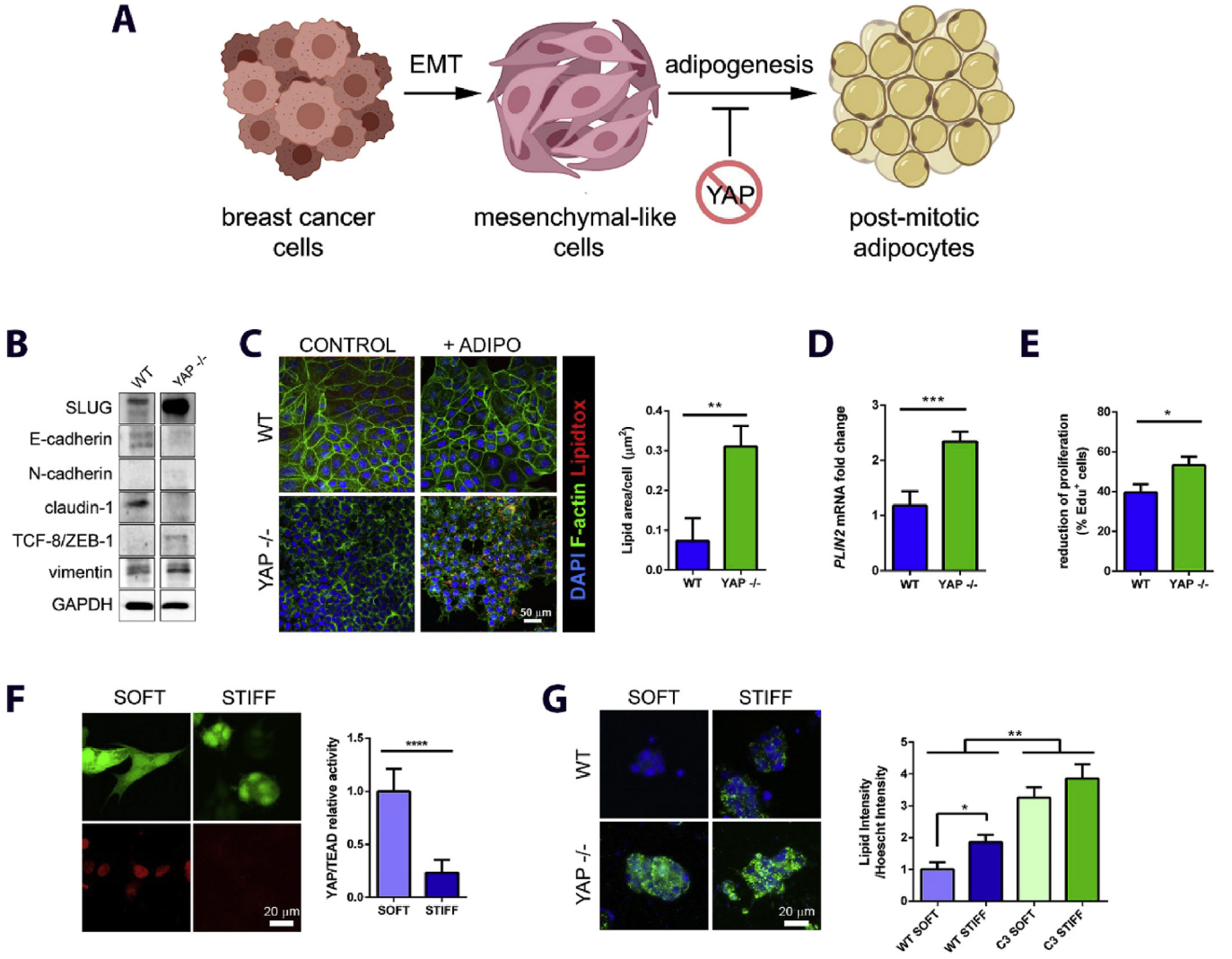

Fig. 7. Cancer-to-adipocyte mechanical reprogramming as a strategy to treat cancer. A. Schematic representation of the experimental design adopted to induce cancer reprogramming into adipocytes through YAP control. **B.** Western blot analysis of the indicated epithelial-to-mesenchymal (EMT) proteins in WT and YAP$^{-/-}$ CAL51 breast cancer cells. **C.** Representative confocal images of WT and YAP$^{-/-}$ CAL51 cells before and after exposure to adipogenic media for 3 days. Cells were stained with DAPI (Blue), F-actin (green) and lipids (LipidTOX, red). Graph: quantification of lipid area per WT and YAP$^{-/-}$ CAL51 cell after adipogenic treatment. **D.** Fold change of the mRNA expression of *PLIN2* adipogenic mRNA in WT and YAP$^{-/-}$ CAL51 cells exposed to adipogenesis media for 3 dayys. The values are normalized to WT. **E.** Reduction in EdU $^{+}$ proliferative cells in WT and YAP$^{-/-}$ CAL51 treated for 3 days with adipogenic medium. The values are expressed as % of positive untreated cells. **F.** Representative confocal images of YAP-TEAD CAL51 mechanoreporter cell line embedded in soft (300 Pa) and stiff (5 KPa) fibrin gels. Graph: quantification of YAP-TEAD transcriptional activity. ****p-value < 0.0001, ***p-vale < 0.001, ** p-value < 0.01, * p-value < 0.05, as calculated by *t*-test analysis.**G.** Representative confocal images of the WT and YAP$^{-/-}$ CAL51 cell line embedded in soft (300 Pa) and stiff (5 KPa) fibrin gels and stimulated for 3 days with adipogenic medium. Cells were stained for lipids (LipidTOX, green) and nuclei (Hoechst). Graph: quantification of LipidTOX intensity in WT and YAP$^{-/-}$ CAL51 cells embedded in soft (300 Pa) and stiff (5 KPa) fibrin gels and stimulated for 3 days with adipogenic medium. The values are expressed as mean intensity normalized by Hoechst intensity in the respective conditions. ** p-value < 0.01, * p-value < 0.05, as determined by one-way ANOVA test followed by Holm-Sidak's multiple comparison. All graphs represent mean ± SD. (For interpretation of the references to colour in this figure legend, the reader is referred to the Web version of this article.)

4.2. The mechanical regulation of adipogenesis through YAP is independent of focal adhesion assembly and cell proliferation

Previous reports implied that adipogenic differentiation requires the rearrangement of cell-ECM discrete contact points, named focal adhesions (FAs) [44,50]. In fact, an augmented cell area correlates with an increased number of FAs [16].

YAP-FA interplay was lately described as the complex result of a feed-forward loop in which YAP localization to the nucleus, being fostered by FA-cytoskeleton stabilization, prompts the transcription of FA genes, thus reinforcing cell-matrix interaction [16,67].

In our experimental setting, a reduction in FA formation obtained by coating the surface with poly-L-lysine (PLL), caused an increase in adipogenesis, probably as a result of cell area being reduced concomitantly [16]. This reduction also prompted a decrease in nuclear YAP.

On the other hand, by exploiting our unique micropatterned fibronectin-coated surfaces controlling the formation of FAs independently of cell area, we were able to rule out the contribution of FA remodeling to MSC adipogenesis.

Our results show that cells having the same area but reduced number of FAs were still not able to accumulate lipid droplets, as a result of YAP co-transcriptional activity still being active [16,61]. Our RNA-seq analysis followed by qPCR on YAP-5SA MSC line confirmed previous data showing that YAP regulates cell adhesion genes [15,16]. The persistent localization of Hippo effector to the nucleus when

adipogenesis is prompted prevents the remodeling of FAs required for cell differentiation.

RNA-seq results also pointed at proliferation as main annotation for YAP co-transcriptional activity, thus confirming previous reports [14,15]. Interestingly, although MSCs progressing to adipogenesis were found to steadily reduce their proliferation capability, this effect was prevented by YAP-5SA expression. Among the genes regulated by YAP hyperactivation in MSCs we found that *CDKN1C* and *CDKN2A* were significantly downregulated. The repression of such genes, which are key controllers of cell cycle progression [68,69] might explain the sustained proliferation of YAP-5SA cells even in the presence of adipogenic stimuli.

The inhibition of cell proliferation in these cells by mitomycin C was not able to restore their adipogenic potential. This result indicates that the blockage of adipogenesis by YAP does not depend on cell proliferation.

4.3. The mechanical regulation of adipogenesis by YAP is independent of TEAD transcription factor

YAP does not bind DNA directly and TEAD transcription factor family (TEAD1-4) is acknowledged of 78% of its transcriptional activity [15].

Nonetheless, few other transcription factors, including RUNX [70], p73 [71], SMAD [72], ERBB4 [11] or β-catenin [8] were found to form transcriptional complexes with YAP. By expressing in MSCs different mutant forms of YAP being able to differentially bind TEAD and the other transcription factors, our experiments show that YAP hyperactivation acts mostly independently of TEAD in the negative regulation of adipogenesis.

In fact, TEAD4 overexpression only mildly reduced adipogenesis while TEAD1 had no effect. Consistently, TEAD4 has been also shown to impact on adipogenesis in a VGLL4/ctBP2-dependent and YAP-independent manner [73].

The specific disruption of YAP-TEAD interaction by pharmacological inhibitor super-TDU also reduced the ability of cells to differentiate, very likely because, by interfering with YAP-TEAD binding, the small molecule makes YAP more available to interact with the other nuclear partners. Among those possible interactors, SMAD proteins [72,74] and β-catenin [75] have been already suggested to act during the osteo/adipo switch.

4.4. Cancer-to-adipocyte reprogramming through the mechanical control of YAP activity

Given the inhibitory effect YAP exerts on MSC adipogenesis and its acknowledged role as oncogene [38,76], we figured the mechanical regulation of YAP transcriptional activity could be exploited to turn tumor cells into non-proliferative fat cells. Cancer-to-adipocyte reprogramming has been lately proposed as a novel approach to the management of malignancies [26].

Our results prove that the mechanical inhibition of YAP activity in breast cancer cells and concomitant adipogenic stimulation can indeed halt tumor cell proliferation and prompt their adipogenic conversion.

Therefore, the mechanical inhibition of YAP in combination with pro-adipogenic drugs (rosiglitazone, trametinib) already available in the market could boost the adipogenic transdifferentiation of cancer cells and improve the effectivity of such therapeutic approaches.

5. Conclusions

In conclusion, our results obtained by single cell analysis, 2D and 3D culture systems highlight the importance of YAP as the mechanoregulated docking protein bringing the mechanical information to the DNA transcription complex. These data pave the way to the design of materials to be exploited in medical applications to control not only mesenchymal stem cell fate downstream of YAP regulation, but also the reprogramming of cancer cells into harmless adipocytes.

Acknowledgements

The work was supported from the European Regional Development Fund in frame of the project Kompetenzzentrum Mechanobiologie (ATCZ133) in the Interreg V-A Austria- Czech Republic programmme. We acknowledge the CF Genomics CEITEC MU supported by the NCMG research infrastructure (LM2015091 funded by MEYS CR) for their support with obtaining scientific data presented in this paper. We are grateful to Vladimir Vinarsky and Federico Tidu for their suggestions regarding the fibrin gels, Jana Bartonova for her technical assistance in FACS and cell sorting, Jana Vasickova for her support with cell culture.

Appendix A. Supplementary data

Supplementary data to this article can be found online at https://doi.org/10.1016/j.biomaterials.2019.03.009.

References

[1] D.E. Discher, P. Janmey, Y.-L. Wang, Tissue cells feel and respond to the stiffness of their substrate, Science (80-.) 310 (2005) 1139–1143, https://doi.org/10.1126/science.1116995.
[2] A.J. Engler, S. Sen, H.L. Sweeney, D.E. Discher, Matrix elasticity directs stem cell lineage specification, Cell 126 (2006) 677–689, https://doi.org/10.1016/j.cell.2006.06.044.
[3] F. Martino, A.R. Perestrelo, V. Vinarský, S. Pagliari, G. Forte, Cellular mechanotransduction: from tension to function, Front. Physiol. 9 (2018) 824, https://doi.org/10.3389/fphys.2018.00824.
[4] G. Forte, F. Carotenuto, F. Pagliari, S. Pagliari, P. Cossa, R. Fiaccavento, A. Ahluwalia, G. Vozzi, B. Vinci, A. Serafino, A. Rinaldi, E. Traversa, L. Carosella, M. Minieri, P. Di Nardo, Criticality of the biological and physical stimuli array inducing resident cardiac stem cell determination, Stem Cell. 26 (2008) 2093–2103, https://doi.org/10.1634/stemcells.2008-0061.
[5] Y.-T. Yeh, S.S. Hur, J. Chang, K.-C. Wang, J.-J. Chiu, Y.-S. Li, S. Chien, Matrix stiffness regulates endothelial cell proliferation through septin 9, PLoS One 7 (2012) e46889, , https://doi.org/10.1371/journal.pone.0046889.
[6] W. Zhong, K. Tian, X. Zheng, L. Li, W. Zhang, S. Wang, J. Qin, Mesenchymal stem cell and chondrocyte fates in a multishear microdevice are regulated by yes-associated protein, Stem Cell. Dev. 22 (2013) 2083–2093, https://doi.org/10.1089/scd.2012.0685.
[7] S. Dupont, L. Morsut, M. Aragona, E. Enzo, S. Giulitti, M. Cordenonsi, F. Zanconato, J. Le Digabel, M. Forcato, S. Bicciato, N. Elvassore, S. Piccolo, Role of YAP/TAZ in mechanotransduction, Nature 474 (2011) 179–183, https://doi.org/10.1038/nature10137.
[8] H. Pan, Y. Xie, Z. Zhang, K. Li, D. Hu, X. Zheng, Q. Fan, T. Tang, YAP-mediated mechanotransduction regulates osteogenic and adipogenic differentiation of BMSCs on hierarchical structure, Colloids Surfaces B Biointerfaces 152 (2017) 344–353, https://doi.org/10.1016/j.colsurfb.2017.01.039.
[9] R. McBeath, D.M. Pirone, C.M. Nelson, K. Bhadriraju, C.S. Chen, Cell shape, cytoskeletal tension, and RhoA regulate stem cell lineage commitment, Dev. Cell 6 (2004) 483–495, https://doi.org/10.1016/S1534-5807(04)00075-9.
[10] L.G. Vincent, Y.S. Choi, B. Alonso-Latorre, J.C. del Álamo, A.J. Engler, Mesenchymal stem cell durotaxis depends on substrate stiffness gradient strength, Biotechnol. J. 8 (2013) 472–484, https://doi.org/10.1002/biot.201200205.
[11] A. Komuro, M. Nagai, N.E. Navin, M. Sudol, WW domain-containing protein YAP associates with ErbB-4 and acts as a co-transcriptional activator for the carboxyl-terminal fragment of ErbB-4 that translocates to the nucleus, J. Biol. Chem. 278 (2003) 33334–33341, https://doi.org/10.1074/jbc.M305597200.
[12] R. Yagi, L.F. Chen, K. Shigesada, Y. Murakami, Y. Ito, A WW domain-containing yes-associated protein (YAP) is a novel transcriptional co-activator, EMBO J. 18 (1999) 2551–2562, https://doi.org/10.1093/emboj/18.9.2551.
[13] Y. Liu-Chittenden, B. Huang, J.S. Shim, Q. Chen, S.-J. Lee, R.A. Anders, J.O. Liu, D. Pan, Genetic and pharmacological disruption of the TEAD-YAP complex suppresses the oncogenic activity of YAP, Genes Dev. 26 (2012) 1300–1305, https://doi.org/10.1101/gad.192856.112.
[14] B. Zhao, K. Tumaneng, K.-L. Guan, The Hippo pathway in organ size control, tissue regeneration and stem cell self-renewal, Nat. Cell Biol. 13 (2011) 877–883, https://doi.org/10.1038/ncb2303.
[15] F. Zanconato, M. Forcato, G. Battilana, L. Azzolin, E. Quaranta, B. Bodega, A. Rosato, S. Bicciato, M. Cordenonsi, S. Piccolo, Genome-wide association between YAP/TAZ/TEAD and AP-1 at enhancers drives oncogenic growth, Nat. Cell Biol. 17 (2015) 1218–1227, https://doi.org/10.1038/ncb3216.
[16] G. Nardone, J. Oliver-De La Cruz, J. Vrbsky, C. Martini, J. Pribyl, P. Skládal, M. Pešl, G. Caluori, S. Pagliari, F. Martino, Z. Maceckova, M. Hajduch, A. Sanz-Garcia, N.M. Pugno, G.B. Stokin, G. Forte, YAP regulates cell mechanics by controlling focal adhesion assembly, Nat. Commun. 8 (2017) 15321, https://doi.org/

10.1038/ncomms15321.
[17] K.M. Kim, Y.J. Choi, J.-H. Hwang, A.R. Kim, H.J. Cho, E.S. Hwang, J.Y. Park, S.-H. Lee, J.-H. Hong, Shear stress induced by an interstitial level of slow flow increases the osteogenic differentiation of mesenchymal stem cells through TAZ activation, PLoS One 9 (2014) e92427, https://doi.org/10.1371/journal.pone.0092427.
[18] D. Mosqueira, S. Pagliari, K. Uto, M. Ebara, S. Romanazzo, C. Escobedo-Lucea, J. Nakanishi, A. Taniguchi, O. Franzese, P. Di Nardo, M.J. Goumans, E. Traversa, P. Pinto-do-Ó, T. Aoyagi, G. Forte, Hippo pathway effectors control cardiac progenitor cell fate by acting as dynamic sensors of substrate mechanics and nanostructure, ACS Nano 8 (2014) 2033–2047, https://doi.org/10.1021/nn4058984.
[19] M. Aragona, T. Panciera, A. Manfrin, S. Giulitti, F. Michielin, N. Elvassore, S. Dupont, S. Piccolo, A mechanical checkpoint controls multicellular growth through YAP/TAZ regulation by actin-processing factors, Cell 154 (2013) 1047–1059, https://doi.org/10.1016/j.cell.2013.07.042.
[20] N.P. Talele, J. Fradette, J.E. Davies, A. Kapus, B. Hinz, Expression of α-smooth muscle actin determines the fate of mesenchymal stromal cells, Stem Cell Rep. 4 (2015) 1016–1030, https://doi.org/10.1016/J.STEMCR.2015.05.004.
[21] Y. An, Q. Kang, Y. Zhao, X. Hu, N. Li, Lats 2 modulates adipocyte proliferation and differentiation via hippo signaling, PLoS One 8 (2013) e72042, , https://doi.org/10.1371/journal.pone.0072042.
[22] A.I. Caplan, *Review:* mesenchymal stem cells: cell–based reconstructive therapy in orthopedics, Tissue Eng. 11 (2005) 1198–1211, https://doi.org/10.1089/ten.2005.11.1198.
[23] A. Oryan, A. Kamali, A. Moshiri, M. Baghaban Eslaminejad, Role of mesenchymal stem cells in bone regenerative medicine: what is the evidence? Cells Tissues Organs 204 (2017) 59–83, https://doi.org/10.1159/000469704.
[24] A. Goldberg, K. Mitchell, J. Soans, L. Kim, R. Zaidi, The use of mesenchymal stem cells for cartilage repair and regeneration: a systematic review, J. Orthop. Surg. Res. 12 (2017) 39, https://doi.org/10.1186/s13018-017-0534-y.
[25] R. Pérez-Cano, J.J. Vranckx, J.M. Lasso, C. Calabrese, B. Merck, A.M. Milstein, E. Sassoon, E. Delay, E.M. Weiler-Mithoff, Prospective trial of Adipose-Derived Regenerative Cell (ADRC)-enriched fat grafting for partial mastectomy defects: the RESTORE-2 trial, Eur. J. Surg. Oncol. 38 (2012) 382–389, https://doi.org/10.1016/J.EJSO.2012.02.178.
[26] D. Ishay-Ronen, M. Diepenbruck, R.K.R. Kalathur, N. Sugiyama, S. Tiede, R. Ivanek, G. Bantug, M.F. Morini, J. Wang, C. Hess, G. Christofori, Gain fat—lose metastasis: converting invasive breast cancer cells into adipocytes inhibits cancer metastasis, Cancer Cell 35 (2019) 17–32, https://doi.org/10.1016/J.CCELL.2018.12.002 e6.
[27] H. Duong, B. Wu, B. Tawil, Modulation of 3D fibrin matrix stiffness by intrinsic fibrinogen-thrombin compositions and by extrinsic cellular activity, Tissue Eng. A 15 (2009) 1865–1876, https://doi.org/10.1089/ten.tea.2008.0319.
[28] J. Zhang, H. Tang, Y. Zhang, R. Deng, L. Shao, Y. Liu, F. Li, X. Wang, L. Zhou, Identification of suitable reference genes for quantitative RT-PCR during 3T3-L1 adipocyte differentiation, Int. J. Mol. Med. 33 (2014) 1209–1218, https://doi.org/10.3892/ijmm.2014.1695.
[29] D. Kim, G. Pertea, C. Trapnell, H. Pimentel, R. Kelley, S.L. Salzberg, TopHat2: accurate alignment of transcriptomes in the presence of insertions, deletions and gene fusions, Genome Biol. 14 (2013) R36, https://doi.org/10.1186/gb-2013-14-4-r36.
[30] S. Anders, P.T. Pyl, W. Huber, HTSeq–a Python framework to work with high-throughput sequencing data, Bioinformatics 31 (2015) 166–169, https://doi.org/10.1093/bioinformatics/btu638.
[31] M.I. Love, W. Huber, S. Anders, Moderated estimation of fold change and dispersion for RNA-seq data with DESeq2, Genome Biol. 15 (2014) 550, https://doi.org/10.1186/s13059-014-0550-8.
[32] G. Yu, L.-G. Wang, Y. Han, Q.-Y. He, clusterProfiler: an R Package for comparing biological themes among gene clusters, OMICS A J. Integr. Biol. 16 (2012) 284–287, https://doi.org/10.1089/omi.2011.0118.
[33] G.R. Warnes, et al., Gplots: Various R Programming Tools for Plotting Data. R Package v.3.0.1, (2016) (n.d.), https://rdrr.io/cran/gplots/.
[34] W. Walter, F. Sánchez-Cabo, M. Ricote, GOplot: an R package for visually combining expression data with functional analysis: fig. 1, Bioinformatics 31 (2015) 2912–2914, https://doi.org/10.1093/bioinformatics/btv300.
[35] S. Kawano, J. Maruyama, S. Nagashima, K. Inami, W. Qiu, H. Iwasa, K. Nakagawa, M. Ishigami-Yuasa, H. Kagechika, H. Nishina, Y. Hata, A cell-based screening for TAZ activators identifies ethacridine, a widely used antiseptic and abortifacient, as a compound that promotes dephosphorylation of TAZ and inhibits adipogenesis in C3H10T1/2 cells, J. Biochem. 158 (2015) 413–423, https://doi.org/10.1093/jb/mvv051.
[36] B. Zhao, X. Wei, W. Li, R.S. Udan, Q. Yang, J. Kim, J. Xie, T. Ikenoue, J. Yu, L. Li, P. Zheng, K. Ye, A. Chinnaiyan, G. Halder, Z.-C. Lai, K.-L. Guan, Inactivation of YAP oncoprotein by the Hippo pathway is involved in cell contact inhibition and tissue growth control, Genes Dev. 21 (2007) 2747–2761, https://doi.org/10.1101/gad.1602907.
[37] B. Zhao, X. Ye, J. Yu, L. Li, W. Li, S. Li, J. Yu, J.D. Lin, C.-Y. Wang, A.M. Chinnaiyan, Z.-C. Lai, K.-L. Guan, TEAD mediates YAP-dependent gene induction and growth control, Genes Dev. 22 (2008) 1962–1971, https://doi.org/10.1101/gad.1664408.
[38] D.D. Shao, W. Xue, E.B. Krall, A. Bhutkar, F. Piccioni, X. Wang, A.C. Schinzel, S. Sood, J. Rosenbluh, J.W. Kim, Y. Zwang, T.M. Roberts, D.E. Root, T. Jacks, W.C. Hahn, KRAS and YAP1 converge to regulate EMT and tumor survival, Cell 158 (2014) 171–184, https://doi.org/10.1016/j.cell.2014.06.004.
[39] T. Oka, M. Sudol, Nuclear localization and pro-apoptotic signaling of YAP2 require intact PDZ-binding motif, Genes Cells 14 (2009) 607–615, https://doi.org/10.1111/j.1365-2443.2009.01292.x.
[40] F. Fan, Z. He, L.-L. Kong, Q. Chen, Q. Yuan, S. Zhang, J. Ye, H. Liu, X. Sun, J. Geng, L. Yuan, L. Hong, C. Xiao, W. Zhang, X. Sun, Y. Li, P. Wang, L. Huang, X. Wu, Z. Ji, Q. Wu, N.-S. Xia, N.S. Gray, L. Chen, C.-H. Yun, X. Deng, D. Zhou, Pharmacological targeting of kinases MST1 and MST2 augments tissue repair and regeneration, Sci. Transl. Med. 8 (2016), https://doi.org/10.1126/scitranslmed.aaf2304 352ra108.
[41] S. Jiao, H. Wang, Z. Shi, A. Dong, W. Zhang, X. Song, F. He, Y. Wang, Z. Zhang, W. Wang, X. Wang, T. Guo, P. Li, Y. Zhao, H. Ji, L. Zhang, Z. Zhou, A peptide mimicking VGLL4 function acts as a YAP antagonist therapy against gastric cancer, Cancer Cell 25 (2014) 166–180, https://doi.org/10.1016/J.CCR.2014.01.010.
[42] C.A. Martz, K.A. Ottina, K.R. Singleton, J.S. Jasper, S.E. Wardell, A. Peraza-Penton, G.R. Anderson, P.S. Winter, T. Wang, H.M. Alley, L.N. Kwong, Z.A. Cooper, M. Tetzlaff, P.-L. Chen, J.C. Rathmell, K.T. Flaherty, J.A. Wargo, D.P. McDonnell, D.M. Sabatini, K.C. Wood, Systematic identification of signaling pathways with potential to confer anticancer drug resistance, Sci. Signal. 7 (2014), https://doi.org/10.1126/scisignal.aaa1877 ra121-ra121.
[43] J.-J. Li, D. Xie, Cleavage of focal adhesion kinase (FAK) is essential in adipocyte differentiation, Biochem. Biophys. Res. Commun. 357 (2007) 648–654, https://doi.org/10.1016/j.bbrc.2007.03.184.
[44] I. Titushkin, S. Sun, A. Paul, M. Cho, Control of adipogenesis by ezrin, radixin and moesin-dependent biomechanics remodeling, J. Biomech. 46 (2013) 521–526, https://doi.org/10.1016/j.jbiomech.2012.09.027.
[45] J. Liu, S.M. DeYoung, M. Zhang, M. Zhang, A. Cheng, A.R. Saltiel, Changes in integrin expression during adipocyte differentiation, Cell Metabol. 2 (2005) 165–177, https://doi.org/10.1016/j.cmet.2005.08.006.
[46] B.C. Low, C.Q. Pan, G. V Shivashankar, A. Bershadsky, M. Sudol, M. Sheetz, YAP/TAZ as mechanosensors and mechanotransducers in regulating organ size and tumor growth, FEBS Lett. 588 (2014) 2663–2670, https://doi.org/10.1016/j.febslet.2014.04.012.
[47] Q.-Q. Tang, T.C. Otto, M.D. Lane, Mitotic clonal expansion: a synchronous process required for adipogenesis, Proc. Natl. Acad. Sci. U.S.A. 100 (2003) 44–49, https://doi.org/10.1073/pnas.0137044100.
[48] M. Reichert, D. Eick, Analysis of cell cycle arrest in adipocyte differentiation, Oncogene 18 (1999) 459–466, https://doi.org/10.1038/sj.onc.1202308.
[49] E.M. Morandi, R. Verstappen, M.E. Zwierzina, S. Geley, G. Pierer, C. Ploner, ITGAV and ITGA5 diversely regulate proliferation and adipogenic differentiation of human adipose derived stem cells, Sci. Rep. 6 (2016) 28889, https://doi.org/10.1038/srep28889.
[50] M. Kuroda, H. Wada, Y. Kimura, K. Ueda, N. Kioka, Vinculin promotes nuclear localization of TAZ to inhibit ECM stiffness-dependent differentiation into adipocytes, J. Cell Sci. 130 (2017) 989–1002, https://doi.org/10.1242/jcs.194779.
[51] I. Stuiver, Z. Ruggeri, J.W. Smith, Divalent cations regulate the organization of integrins αvβ3 and αvβ5 on the cell surface, J. Cell. Physiol. 168 (1996) 521–531, https://doi.org/10.1002/(SICI)1097-4652(199609)168:3<521::AID-JCP4>3.0.CO;2-R.
[52] M. Shimaya, T. Muneta, S. Ichinose, K. Tsuji, I. Sekiya, Magnesium enhances adherence and cartilage formation of synovial mesenchymal stem cells through integrins, Osteoarthritis Cartilage 18 (2010) 1300–1309, https://doi.org/10.1016/J.JOCA.2010.06.005.
[53] T.P. Driscoll, B.D. Cosgrove, S.J. Heo, Z.E. Shurden, R.L. Mauck, Cytoskeletal to nuclear strain transfer regulates YAP signaling in mesenchymal stem cells, Biophys. J. 108 (2015), https://doi.org/10.1016/j.bpj.2015.05.010.
[54] K.C. Lin, T. Moroishi, Z. Meng, H.-S. Jeong, S.W. Plouffe, Y. Sekido, J. Han, H.W. Park, K.-L. Guan, Regulation of Hippo pathway transcription factor TEAD by p38 MAPK-induced cytoplasmic translocation, Nat. Cell Biol. 19 (2017) 996–1002, https://doi.org/10.1038/ncb3581.
[55] S.R. Caliari, S.L. Vega, M. Kwon, E.M. Soulas, J.A. Burdick, Dimensionality and spreading influence MSC YAP/TAZ signaling in hydrogel environments, Biomaterials 103 (2016) 314–323, https://doi.org/10.1016/j.biomaterials.2016.06.061.
[56] A. Elosegui-Artola, R. Oria, Y. Chen, A. Kosmalska, C. Pérez-González, N. Castro, C. Zhu, X. Trepat, P. Roca-Cusachs, Mechanical regulation of a molecular clutch defines force transmission and transduction in response to matrix rigidity, Nat. Cell Biol. 18 (2016) 540–548, https://doi.org/10.1038/ncb3336.
[57] S.T. Coffin, G.R. Gaudette, Aprotinin extends mechanical integrity time of cell-seeded fibrin sutures, J. Biomed. Mater. Res. A. 104 (2016) 2271–2279, https://doi.org/10.1002/jbm.a.35754.
[58] J.P. Winer, S. Oake, P.A. Janmey, Non-linear elasticity of extracellular matrices enables contractile cells to communicate local position and orientation, PLoS One 4 (2009) e6382, https://doi.org/10.1371/journal.pone.0006382.
[59] G.S. Baia, O.L. Caballero, B.A. Orr, A. Lal, J.S.Y. Ho, C. Cowdrey, T. Tihan, C. Mawrin, G.J. Riggins, Yes-associated protein 1 is activated and functions as an oncogene in meningiomas, Mol. Canc. Res. 10 (2012) 904–913, https://doi.org/10.1158/1541-7786.MCR-12-0116.
[60] T. Tchkonia, T. Thomou, Y. Zhu, I. Karagiannides, C. Pothoulakis, M.D. Jensen, J.L. Kirkland, Mechanisms and metabolic implications of regional differences among fat depots, Cell Metabol. 17 (2013) 644–656, https://doi.org/10.1016/j.cmet.2013.03.008.
[61] W. Qian, L. Gong, X. Cui, Z. Zhang, A. Bajpai, C. Liu, A.B. Castillo, J.C.M. Teo, W. Chen, Nanotopographic regulation of human mesenchymal stem cell osteogenesis, ACS Appl. Mater. Interfaces 9 (2017) 41794–41806, https://doi.org/10.1021/acsami.7b16314.
[62] H.S. Frederick, G. Hamel, J.S.L. Ligyeom Ha, J.S. Lee, L. Ha, J.Y. Lim, Mechanical control of mesenchymal stem cell adipogenesis, Endocrinol. Metab. Syndrome 04 (2015), https://doi.org/10.4172/2161-1017.1000152.
[63] K. Kamura, J. Shin, H. Kiyonari, T. Abe, G. Shioi, A. Fukuhara, H. Sasaki, Obesity in Yap transgenic mice is associated with TAZ downregulation, Biochem. Biophys. Res. Commun. 505 (2018) 951–957, https://doi.org/10.1016/J.BBRC.2018.10.037.
[64] S. Khetan, M. Guvendiren, W.R. Legant, D.M. Cohen, C.S. Chen, J.A. Burdick,

Degradation-mediated cellular traction directs stem cell fate in covalently cross-linked three-dimensional hydrogels, Nat. Mater. 12 (2013) 458–465, https://doi.org/10.1038/nmat3586.
[65] O. Chaudhuri, L. Gu, D. Klumpers, M. Darnell, S.A. Bencherif, J.C. Weaver, N. Huebsch, H.-P. Lee, E. Lippens, G.N. Duda, D.J. Mooney, Hydrogels with tunable stress relaxation regulate stem cell fate and activity, Nat. Mater. 15 (2016) 326–334, https://doi.org/10.1038/nmat4489.
[66] A. Das, R.S. Fischer, D. Pan, C.M. Waterman, YAP nuclear localization in the absence of cell-cell contact is mediated by a filamentous actin-dependent, myosin II- and phospho-YAP-independent pathway during extracellular matrix mechanosensing, J. Biol. Chem. 291 (2016) 6096–6110, https://doi.org/10.1074/jbc.M115.708313.
[67] B.M. Gumbiner, N.-G. Kim, The Hippo-YAP signaling pathway and contact inhibition of growth, J. Cell Sci. 127 (2014) 709–717, https://doi.org/10.1242/jcs.140103.
[68] K. Wouters, Y. Deleye, S.A. Hannou, J. Vanhoutte, X. Maréchal, A. Coisne, M. Tagzirt, B. Derudas, E. Bouchaert, C. Duhem, E. Vallez, C.G. Schalkwijk, F. Pattou, D. Montaigne, B. Staels, R. Paumelle, The tumour suppressor CDKN2A/p16 ^{INK4a} regulates adipogenesis and bone marrow-dependent development of perivascular adipose tissue, Diabetes Vasc. Dis. Res. 14 (2017) 516–524, https://doi.org/10.1177/1479164117728012.
[69] A. Matsumoto, S. Takeishi, T. Kanie, E. Susaki, I. Onoyama, Y. Tateishi, K. Nakayama, K.I. Nakayama, p57 is required for quiescence and maintenance of adult hematopoietic stem cells, Cell Stem Cell 9 (2011) 262–271, https://doi.org/10.1016/j.stem.2011.06.014.
[70] A. Passaniti, J.L. Brusgard, Y. Qiao, M. Sudol, M. Finch-Edmondson, Roles of RUNX in hippo pathway signaling, Adv. Exp. Med. Biol. (2017) 435–448, https://doi.org/10.1007/978-981-10-3233-2_26.
[71] S. Strano, E. Munarriz, M. Rossi, L. Castagnoli, Y. Shaul, A. Sacchi, M. Oren, M. Sudol, G. Cesareni, G. Blandino, Physical interaction with yes-associated protein enhances p73 transcriptional activity, J. Biol. Chem. 276 (2001) 15164–15173, https://doi.org/10.1074/jbc.M010484200.
[72] O. Ferrigno, F. Lallemand, F. Verrecchia, S. L'Hoste, J. Camonis, A. Atfi, A. Mauviel, Yes-associated protein (YAP65) interacts with Smad 7 and potentiates its inhibitory activity against TGF-β/Smad signaling, Oncogene 21 (2002) 4879–4884, https://doi.org/10.1038/sj.onc.1205623.
[73] W. Zhang, J. Xu, J. Li, T. Guo, D. Jiang, X. Feng, X. Ma, L. He, W. Wu, M. Yin, L. Ge, Z. Wang, M.S. Ho, Y. Zhao, Z. Fei, L. Zhang, The TEA domain family transcription factor TEAD4 represses murine adipogenesis by recruiting cofactors VGLL4 and CtBP2 into a transcriptional complex, J. Biol. Chem. (2018), https://doi.org/10.1074/jbc.RA118.003608 jbc.RA118.003608.
[74] L. Choy, R. Derynck, Transforming growth factor-beta inhibits adipocyte differentiation by Smad 3 interacting with CCAAT/enhancer-binding protein (C/EBP) and repressing C/EBP transactivation function, J. Biol. Chem. 278 (2003) 9609–9619, https://doi.org/10.1074/jbc.M212259200.
[75] J.-X. Pan, L. Xiong, K. Zhao, P. Zeng, B. Wang, F.-L. Tang, D. Sun, H. Guo, X. Yang, S. Cui, W.-F. Xia, L. Mei, W.-C. Xiong, YAP promotes osteogenesis and suppresses adipogenic differentiation by regulating β-catenin signaling, Bone Res. 6 (2018) 18, https://doi.org/10.1038/s41413-018-0018-7.
[76] D. Pan, The hippo signaling pathway in development and cancer, Dev. Cell 19 (2010) 491–505, https://doi.org/10.1016/j.devcel.2010.09.011.